Green Production of Microelectronics-Grade Hydrogen and Research-Grade Oxygen

A Technical Report submitted to the Department of Chemical Engineering

Presented to the faculty of the School of Engineering and Applied Sciences

University of Virginia • Charlottesville, Virginia

In Partial Fulfillment of the Requirements for the Degree

Bachelor of Science, School of Engineering and Applied Science

Spring, 2024

Technical Project Team Members

Amara Pettit

Daniel Sweeney III

Brian Song

Abhinav Sanjay

Amish Madhav

On my honor as a University Student, I have neither given nor received unauthorized aid on this assignment as defined by the Honor Guidelines for Thesis-Related Assignments

Eric Anderson, Department of Chemical Engineering

Table of Contents

Executive Summary

This paper describes the design of the plant which produces microelectronic grade green hydrogen, and research-grade oxygen as a coproduct. The design incorporates Aspen Plus v14 modeling, adsorption equilibrium data, and a life cycle economic analysis of the plant. The motivation for this plant is to provide a clean and sustainable way to produce hydrogen gas for the microelectronics industry to reduce carbon footprint and environmental impacts of the hydrogen production industry, currently dominated by gray production processes.

The process begins with the purification of river water to create a suitable inlet for high-purity green hydrogen production. The water is first run through a coarse filter to remove large debris present in the river. Then, the water is put through a rapid sand filter, to remove smaller suspended particles, a UV disinfection tube, to kill and present bacteria and algae, and a Granulated Activated Carbon (GAC) filter, to remove organic contaminants. This water is further purified by a reverse osmosis (RO) unit, heated to 25^{o}C temperature, and fed to the PEM electrolyzer.

The electrolyzer splits the water into hydrogen (H_2) and oxygen (O_2) gas, which are then sent to downstream purification processes. The gasses first encounter, in separate processes, a condenser to remove the majority of water vapor picked up in the electrolyzer. Then, the gasses are sent to a pressure swing adsorption (PSA) column, to remove further impurities. The hydrogen and oxygen separation processes use 5A and 13X zeolite, respectively. After sending the gasses through a multistage compression and bottling process, the hydrogen gas is ready to be sold to the microelectronics industry and the oxygen gas to the research industry, both at 99.999% purity.

The plant is designed to operate for 8,000 hours a year, producing 1,864,000 kg of hydrogen per year and 15,334,000 kg of oxygen per year. This gives a yearly hydrogen revenue of $394,413,880.66 and an oxygen revenue of $45,109,684.35. The plant's costs include a $34 million equipment cost, $202 million capital cost, $400,000 yearly material cost, $4.5 million yearly utility cost, and a total yearly operating cost of $15 million. After conducting a 20 year economic analysis on the lifetime of the plant, using a 10-year straight line depreciation, the internal rate of return (IRR) was found to be 64%, and expected revenue at 6.6 billion dollars. Additionally, because the IRR value is greater than the estimated hurdle discount rate of 18%, we can conclude that this process is economically feasible. Therefore, we believe that this project should be executed because it is entirely carbon-neutral, beneficial for the environment, and ultimately a financial success.

1. Introduction

1.1 Background

Hydrogen is a crucial part of our current economy, playing large roles in fertilizer production, semiconductors, and fuel cell use. Its role in fertilizer production cannot be understated, with over half of all hydrogen produced being used in the Haber-Bosch process to create ammonia (AIChE, 2019). Fuel cells may also serve as a potential future use of hydrogen. This has attracted particular interest as they would provide carbon-neutral electricity without requiring recharging, making this technology particularly attractive for car usage (U.S. Department of Energy, n.d). Lastly, hydrogen presents a large variety of uses in the electronics industry, where it is used for both heat transfer capabilities and as a reducing and etching agent (Cigal, n.d.). Therefore, as the modern world's dependence on electronics continues to expand, it is essential to optimize the production of hydrogen.

Unfortunately, the cheapest and most common method of hydrogen production is sourced from fossil fuels ("gray hydrogen"). This process uses steam methane reformation with a water-gas shift reaction, consequently releasing dangerous levels of greenhouse gasses. As concerns regarding climate change grow, it becomes increasingly important to invest in technologies that reduce global carbon footprints. Production of green hydrogen mitigates this environmental challenge by using renewable energy sources (such as wind and solar) to perform water electrolysis, generating hydrogen and providing a carbon-free process to meet our economies' hydrogen needs.

However, currently, green hydrogen's largest barrier to implementation is cost, priced at over four times that of gray hydrogen (BloombergNEF, 2023). Our process utilizes byproducts of electrolysis to increase profits by selling co-produced oxygen at research-grade. Additionally, the

electronics industry is the optimal consumer of hydrogen because of its highest-value market price. These strategies ensure that our green hydrogen process satisfies global electronic needs, economically viable, and environmentally friendly.

1.2 Product Overview

In this process, ultrapure hydrogen and research-grade oxygen are produced by the electrolysis of water. The chemical formulas of the products are H_2 and O_2, respectively. The intended market for our hydrogen product is the semiconductor and microelectronics industries, which require a minimum of 99.999% purity (Process Sensing Technologies, n.d.). This also requires that gas contaminations below the thresholds of than 2 ppm CO_2, 2 ppm CO, 2 ppm N_2, 1 ppm O_2, and 3.5 ppm water (Smith, n.d.). The intended market for our oxygen product is the research industry, which is globally regulated by the World Health Organization (WHO). Currently our process aims to reach a minimum of 99.999% oxygen purity, ensuring less than 1 ppm CO_2, 1 ppm CO, 4 ppm N_2, and 1 ppm H_2O (CO_2 Meter., n.d.). The hydrogen and oxygen products will be bottled in 250 L gas cylinders and sold at 70 MPa and 15.2 MPa, respectively.

1.3 Starting Materials

There is no recordable data of the water composition specifically for Lake Torneträsk or the water just downstream in the Torne River, so the composition was estimated using data collected from the River Torne watersheds and other northern Nordic river systems.
Table 1-3-01 below shows the chemical data (pH, alkalinity, total organic carbon, phosphorus, and nitrogen) collected for seven River Torne watersheds between 2004-2005. The chemical properties of the input water to our process were estimated by taking the average values of these

seven watersheds. Using this estimation, our input water has a neutral pH of 7.05, a TOC content of 1.36 mg/L, 5.43 µg/L phosphorus, and 150 µg/L nitrogen (Länsstyrelsen., n.d.).

These estimations are comparable to the values recorded in a separate study of 20 Nordic rivers between 2013-2017 (Mean pH = 7.01, TOC = 2.68 mg/L, phosphorus = 6.38 µg/L, nitrogen = 291 µg/L). The two rivers Alna and Orreevla were excluded from mean calculations because their water content is influenced significantly by nearby urban areas and agricultural activity; these are not influences that affect Abisko where our plant is located (NIWA, n.d.). Given the similarities in results between the two studies, further chemical characterization of our input water was made using this second study of Norwegian rivers. The mean values of the data can be seen in Table 1-3-02 below.

Table 1-3-01. Chemical Properties and Phytoplankton Status for the River Torne Northern Highland Watersheds and Torne River Estimation

Lake	pH	Total Organic Carbon (mg/L)	Total Phosphorus (µg/L)	Total Nitrogen (µg/L)	Total Season Mean Bacteria Volume (µg/L)	Cyanobacteria Volume in August (µg/L)
Partaljaure	6.85	1.5	5	130	69	0
Saanaharvi	7.1	1.5	5	147	74	0.3
Tjalmejaure	7.21	1.5	6	140	149	0.9
Toskal Jarvi	7.49	0.7	6	90	65	0
Aggojaure	7.17	2.1	7	137	125	2
Latnjajaure	6.41	0.7	3	207	55	0
Abiskojaure	7.12	1.5	6	201	55	0
Average (estimate near Abisko)	7.05	1.36	5.43	150	85	0.46

Table 1-3-02. Torne River Chemical Characterization Using Mean Values of Norwegian Rivers

Component	Concentration (mg/L)
Suspended particulate matter	2.61
Calcium	2.
Silica	2.94
Arsenic	1.3e-4
Lead	2.1e-4
Cadmium	1.5e-6
Copper	1.1e-3
Zinc	3.1e-3
Chromium	2.5e-4
Nickel	5.0e-4

1.4 Scale

1.4.1 Microelectronics-Grade Hydrogen

To determine the scale of this project, the market size for green hydrogen in the microelectronic industry was analyzed. Globally, this industry has been estimated to reach $3.6 billion by 2030 (AIER, 2024), and our goal is to control 10% of this market (generating around 360 million dollars in revenue from hydrogen). However, overestimates of product loss in initial purification calculations resulted in our plant producing around 10.9% of the market, equaling a hydrogen revenue of $394,413,880.66, 15,334,000 kg, and 1,538,400 bottles produced yearly.

1.4.2 Research-Grade Oxygen

As a byproduct of electrolysis, the scale of research-grade oxygen is set through the hydrogen's production goals. Therefore, this plant produces or 1,864,000 kg of oxygen yearly bottled within 36,550 gas cylinders, generating $45,109,684.35 in revenue.

2. Discussion

Water will be pumped directly from the Torne River to our green hydrogen plant. The water will be purified by a pretreatment system containing a coarse filter, rapid sand filter, ultraviolet disinfection, granular activated carbon (GAC) filter, and reverse osmosis (RO) unit. All contaminants except dissolved gasses such as carbon dioxide (CO_2), nitrogen (N_2), and oxygen (O_2) are removed from the water before being sent to a PEM electrolyzer where the water is split into hydrogen and oxygen. The outlet hydrogen and oxygen streams from the electrolyzer will contain dissolved gas contaminants mentioned above and water vapor (H_2O). The condenser units will condense the majority of the water impurities to be recycled back into the electrolyzer. The hydrogen and oxygen streams will then pass through pressure swing adsorption units, which will purify them to over 99.999%. These purified products will be compressed to be stored and shipped to buyers. In the discussion section below, it is broken into four major sections: water purification, PEM electrolysis, hydrogen purification and oxygen purification. The overall block flow diagram for this process is shown in Figure 2-0-01 below.

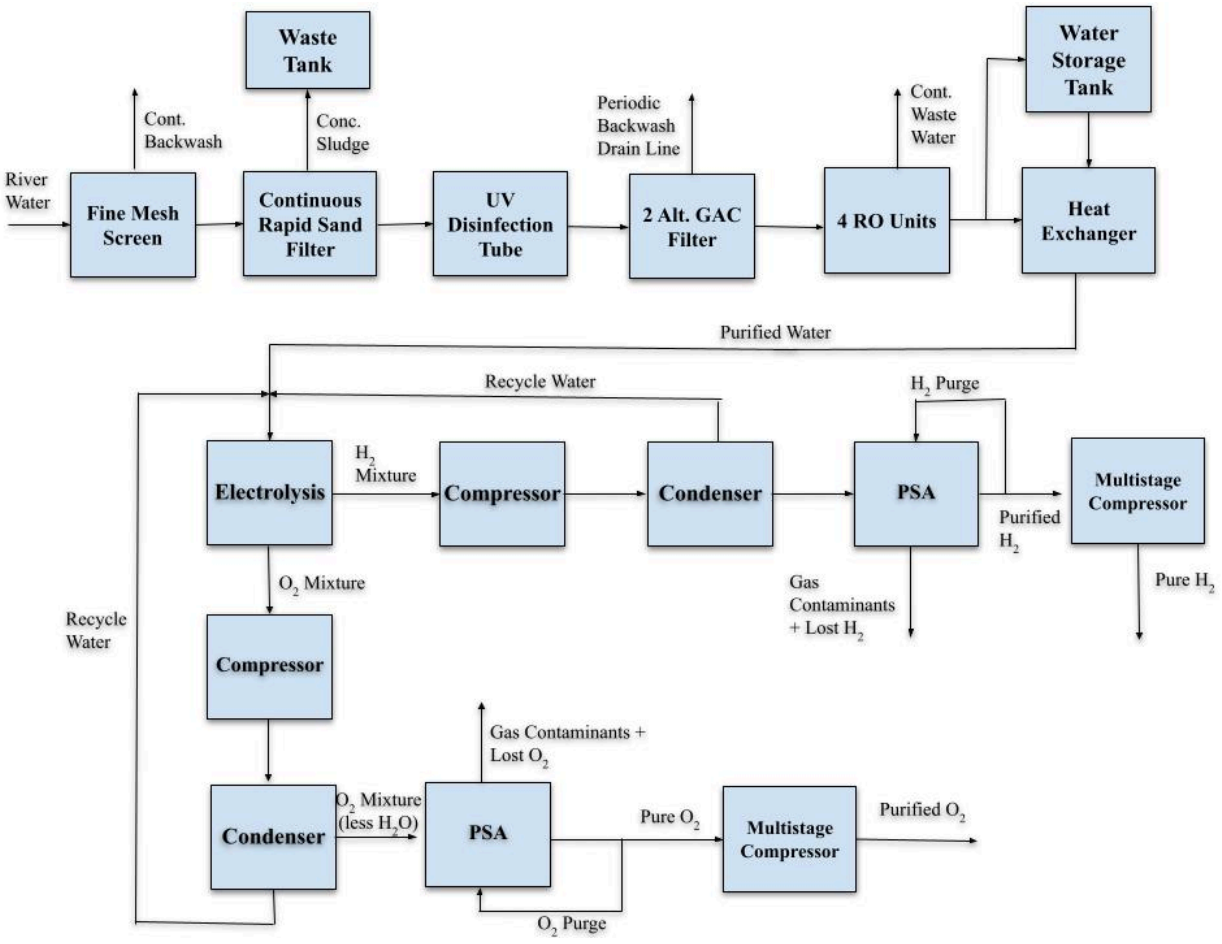

Figure 2-0-01. Block Flow Diagram for Green Hydrogen Plant

2.1 Plant Location

Our plant will be located in Abisko, Sweden, co-locating with a microelectronics producer for easy access to our hydrogen. We chose Sweden because the most significant cost to our plant was the energy costs, and Sweden offers inexpensive wind energy compared to other places in the world. Our specific chemical processing facility will be erected on 27 acres of land, based off of a Swedish water processing facility with similar processing capacities (Heat Pumping Technologies, n.d.). Abisko is the ideal location for our plant for several reasons. First, Abisko is a low-resident town with an abundance of available land for development. Second, it is

right beside Lake Torneträsk, an open lake that is believed to be the primary water source for the Torne River. This is extremely convenient for our water-centric process. Third, the Torne River has the highest salinity at the downstream estuary near the Gulf of Bothnia and has a decreasing salinity as you move upstream. Abisko is located upstream of the Torne River, so the water we will be sourcing for our process will have a low salinity and require less pretreatment.

Figure 2-1-01: Green Hydrogen Plant Location (Google Earth, n.d.)

One key issue we addressed before process design was the potential for the lake or river to freeze entirely, which would cut off our supply of water. Abisko has an average annual temperature of -1.7 °C (29.0 °F) and experiences a significant amount of rainfall (1012 mm per year) (Climate Data, n.d.). Due to the low temperatures, Lake Torneträsk and the Torne River are typically frozen between December and May. The ice thickness of the Torne River has been measured at the observation site in Tornio since 1964, most frequently on 30 March, and found that the mean thickness during the period 1964–2019 was 76.5 cm (Norrgård & Helama, 2022). On average, Abisko is ~3.0 °C colder than Tornio year-round, so the mean ice thickness is

expected to be slightly greater than 76.5 cm (Climate Data, n.d.). However, Lake Torneträsk has a maximum depth of 168 m and the Torne River has a maximum depth of 294 m. Both Lake Torneträsk and the Torne River are large sources of water, so we are confident there will be plenty of fresh flowing water even during the coldest months of January and February.

2.2 Water Pretreatment Design

2.2.1 Coarse Mesh Screen

When sourcing water from natural bodies of water, it is important to remove large impediments such as algae, leaves, moss, sticks, small rocks, or fish in order to protect the inlet pump and downstream water purification units from clogging and will extend their lifetimes. It is common to see either a screen around the pump or a filter membrane at the entrance of the pipe. Our team decided to implement the coarse mesh screen around the pump. No calculations or estimations were made for the concentration of large impediment content within the river water because the screen is "self cleaning," meaning it has a continuous backwashing system that prevents contaminant build-up on the filter's surface.

For this step, we will be using the RF-100 Pump (Rotorflush, n.d.) seen in Figure 2-2-1-01 below. There were multiple screen sizes to choose from: 100 µm and 250 µm. The 250 µm was chosen in order to support the required flow rates for our process. The 250 µm version can process up to 3,593 kg/hr of water. Our process requires 8994.8 kg/hr of water during normal operations and 13,258 kg/hr of water during GAC and coarse filter backwashing. In order to accommodate our maximum 13,258 kg/hr of water demand, we need four RF100 Duplex Pump Self-Cleaning Filters. For redundancy and in case of unexpected maintenance or errors, a fifth unit will be installed.

The filter's mesh is made of a nylon material that degrades over time and it is recommended that they be replaced or cleaned with water and detergent every 5000 hours of use. Given this recommendation, each filter will be cleaned with water and detergent during summer shutdown in July and each filter will be replaced during end-of-year shutdown in December.

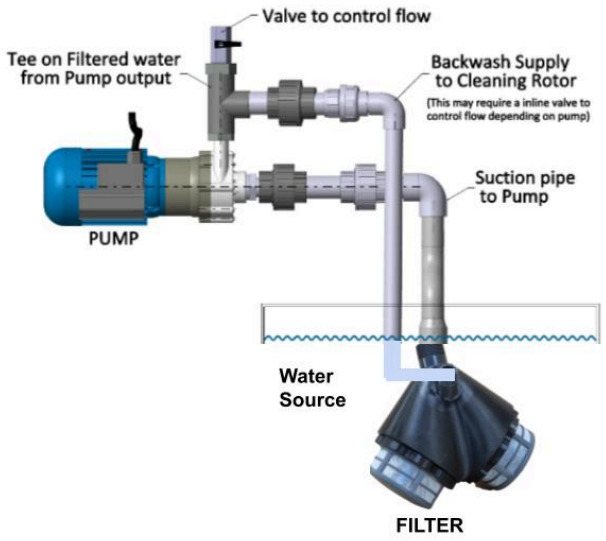

Figure 2-2-1-01: Image of Coarse Mesh Screen Apparatus (Rotorflush, n.d.)

2.2.2 Rapid Sand Filter

After the coarse mesh screen, the water passes through a rapid sand filter. Sand filters are used to remove suspended particulate matter (SPM). By decreasing the turbidity of the river water, we reduce the probability of downstream clogging of filters such as GAC and RO. The two types of sand filters are slow and fast sand filters. Rapid sand filters use fine sand and high flow rates for quicker water purification, while slow sand filters employ coarser sand and lower flow rates, relying on biological processes. Rapid filters are more efficient but require more maintenance, whereas slow sand filters are simpler and naturally self-cleaning (1-2 days versus 3-4 months. Since our process requires a relatively high flow rate of up to 10606 kg/hr water

during GAC backwashing, our team decided to proceed with the rapid sand filter, specifically the The Parkson DynaSand® Filter (Parkson, n.d.) seen in Figure 2-2-2-01 below.

As seen in Table 1-3-02, the input water is estimated to contain 2.61 mg/L of SPM, which is equivalent to a turbidity of 7.83 NTU. The Parkson DynaSand Filter is capable of purifying a stream from 10 NTU to 0.1 NTU (99% efficient). Since 7.83 NTU is similar in magnitude to 10 NTU, we assumed a similar efficiency for our system. The remaining 1% of SPM impurities will be removed by later water purification steps. This filter will have a fiberglass-reinforced plastic (FRP) shell. This was chosen over 304 stainless steel and carbon steel shells because FRP is cheaper and is just as resistant to corrosion. To calculate the required filter cross-sectional area, we divided the inlet flow rate during normal operations (7,195 kg/hr) by the loading rate of 9,779 $kg/hr/m^2$ (4 $gal/min/ft^2$) found in the manual and obtained a cross-sectional area of 0.73 m^2. During backwashing of GAC, the inlet flow rate to the sand filter will temporarily increase to 10606 kg/hr, which will change the loading rate to 14,529 $kg/hr/m^2$ (5.94 $gal/min/ft^2$), which is within the loading capacity limits of this instrument.

Many sand filter systems require additional coagulation or flocculation steps that encourage the SPM to clump together to make them easier to remove. The Parkson DynaSand® Filter utilizes a proprietary process known as Continuous Contact Filtration that performs coagulation and flocculation within the sand bed, eliminating the need for external flocculators and clarifiers. It is best suited to remove small floc, which can help reduce chemical requirements by 20-30% over conventional treatment. Given this, no additional design of coagulation or flocculation were performed.

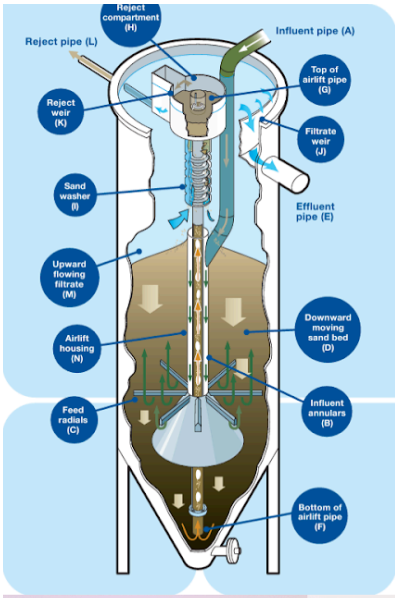

Figure 2-2-2-01: Image of Continuous Rapid Sand Filter (Parkson, n.d.)

2.2.3 Waste Tank

The SPM that is filtered out of the rapid sand filter will be a 1:1 slurry of the removed suspended particles and water. This waste will be collected in a holding tank that will be disposed of at an off-site landfill. Our team decided to empty the tank and dispose of the waste on the 28th of each month. The suspended particulate matter filtered out by the rapid sand filter exits at 0.037 kg/hr under normal operations and 0.055 kg/hr during GAC backwash. There will be about 10 GAC backwashes per month with each lasting 20 min, so one month's operation will result in about 30 kg SPM/water waste. Assuming density of the sludge is the same as water, we will be installing a 37.85 L (10 gallon) stainless steel tank for this unit.

2.2.4 UV Disinfection

After the rapid sand filter, the water will be passed through a UV disinfection tube to kill the live bacteria that could cause biofouling and deteriorate the GAC and RO membranes.

As seen in Table 1-3-01, the mean annual volume of bacteria is 85 µg/L and the concentration of cyanobacteria is estimated to be 0.46 µg/L. Figure 2-2-4-0 shows the Polaris Scientific UVA-60B product (US Water Systems, n.d.) we will be using. It can kill up to 99.99% of these live contaminants using 5 LED lamps that emit a wavelength of 254 nm. The 304 stainless steel tube has dimensions of 13.9 cm x 93.8 cm (5.5 in x 36.93 in) and has a maximum capacity of 13,627 kg/hr (60 GPM) of water, which is sufficient for our maximum required flow rate of 10606.82 kg/hr of water during GAC backwash. Therefore, the target residence time is ~3.8 sec. The dead cell-debris will then be filtered out by either the GAC filter or the RO system.

Figure 2-2-4-01: Image of UV Disinfection Instrument (US Water Systems, n.d.)

This product has a rated life of 9,000 hours. Our plant will be operating at about 8,000 hours per year, so the UV disinfection tube lamps will be replaced during the end-of-year shutdown in December.

2.2.5 GAC Filter

After UV disinfection, the water is sent through a granular activated carbon (GAC) filter, which is used to remove organic contaminants such as chlorine, iron, hydrogen sulfide, heavy metals via redox reactions.

As seen in Table 1-3-02, the TOC content was found to be 1.36 mg/L. We are assuming that the GAC filter will remove over 99% of the organic contaminants. We will be using the Crystal Quest® Commercial Granular Activated Carbon (GAC) Filters (Crystal Quest Water Filters, n.d.) shown in Figure 2-2-5-01. The service flow rate of this product during normal operations is 32,800 kg/hr/m^2 (15 gal/min/ft^2). Since we need to process 7,195 kg/hr water under normal operations, the GAC filter will have a cross-sectional area of 0.22 m^2. The Crystal Quest requires non-continuous backwashing to clean the filter's membrane, so two GAC filter units will be installed and they will be alternated every three days to perform backwashing. The backwashing process only takes 20 minutes and the flow rate is temporarily increased to 10,606 kg/hr water in order to support both the production minimum flow rate of 7,195 kg/hr and the required backwashing flow rate of 3,411 kg/hr. During backwashing, the loading rate increases to 48,209 kg/hr/m^2 (19.3 gal/min/ft^2) which is within the operating limits of this instrument. The backwashed water will exit out of a drain line, pumped and released to the nearby river.

Figure 2-2-5-01: Image of GAC Filter (Crystal Quest Water Filters, n.d.)

2.2.6 Reverse Osmosis and Water Storage Tank

After GAC, the water is sent through a reverse osmosis (RO) system (Crystal Quest Water Filters, n.d.) to remove any of the remaining contaminants. The RO unit shown in Figure 2-2-6-01 has an efficiency that ranges from 33% to 50%. Given the extensive pretreatment of the water prior to RO it is expected that the efficiency will be closer to 50%, but for the purposes of over designing and being conservative, we assumed an efficiency of 33%. Using this efficiency, our process requires an input flow rate of 7195 kg/hr of water into the RO system. To accommodate this, we will be installing four RO units in parallel that each have a maximum capacity of 6,548 kg/hr of water and 14 membranes. Two RO units will be operational at a time. On the 28th of each month (also when the GAC filters are swapped), the RO units will be swapped for cleaning and maintenance. With proper maintenance, these RO units are expected to last 4 years.

The water storage tank is another level of redundancy. It is designed to hold 4 hours' worth of purified water in case there are any unexpected issues with the water pretreatment system. During the start-up process, the water storage tank will be filled with 9.53 m^3 of purified water. This will be held in a 10,000 liter carbon steel tank. Once this target is hit, the valve on stream 12 and stream 10 will open and the process will run continuously, feeding the heat exchanger a steady 2374 kg/hr of water.

Figure 2-2-6-01: Image of RO System (Crystal Quest Water Filters, n.d.)

2.3 Electrolysis Design

2.3.1 Electrolyzer Type

One of the first considerations for electrolysis before getting into design parameter engineering is the type of electrolyzer for the process. Given our main goal for the process is to produce high-purity hydrogen at commercial volumes, we compared reported and short-term projections of performance for different electrolyzer technologies in the context of our design criteria. There are four types of electrolyzers we considered: alkaline water electrolyzers (AWE), anion-exchange membrane (AEM) water electrolyzers, solid oxide water electrolyzers (SOE), and proton-exchange membrane (PEM) water electrolyzers.

2.3.1.1 Alkaline water electrolyzers

Alkaline water electrolyzers (AWEs) are the current choice for many industrial applications of hydrogen production. As Kumar and Lim report, established players in the field such as Cummins from Canada, Sunfire from Germany, and GreenHydrogen from Denmark all leverage alkaline water electrolysis for their hydrogen production (2022). AWE is a relatively mature technology compared to the other electrolysis methods and thus has benefits associated with that longer-term development. AWE does not require noble metals for electrodes which significantly reduces costs, and many commercial demonstrations have shown long lifespans of hydrogen production (Kumar and Lim, 2022). However, the biggest drawback with alkaline water electrolysis is the lowest current density (0.1-0.5 A/cm^2) among active electrolyzer technologies (Emam et al., 2024). Current density directly affects the amount of water that is able to be electrolyzed, and thus, the amount of hydrogen that can be produced. Low current

density is a significant bottleneck for our process given the volume of hydrogen we are aiming to produce. While research on better electrode and membrane performance could improve performance, we do not feel that alkaline water electrolyzers are suitable for our process.

2.3.1.2 Anion-exchange membrane water electrolyzers

Anion-exchange membrane water electrolyzers are another interesting choice for hydrogen reaction. This technology is primarily in research and development, but has the potential to address the low current density issue of alkaline water electrolysis without adding too much in cost, while offering up to 10% additional improvement in energy-to-production efficiency (Kumar and Lim, 2022). However, commercial applications of AEM electrolysis have not been demonstrated as of yet, and there is simply a lack of data available to make large-scale designs for long-lifespan AEM plants (Xu et al., 2022). While this technology could be worth revisiting given developments in AEM research, it is not feasible for commercial design at present.

2.3.1.3 Solid oxide water electrolyzers

Solid oxide water electrolysis is one technology we considered, but it is also in developmental stages and has a similar design outlook to AEM electrolysis as mentioned previously. The attraction of SOE is in its high energy-to-production efficiency (80%-90%) and potentially low cost of material construction (Emam et al., 2024). Again, a lack of implementation at commercial scale combined with inadequate design data make it impractical to suggest any plant setups with SOE at present, but it should be a technology that is revisited once it reaches larger-scale viability.

`

2.3.1.4 Proton-exchange membrane electrolyzers

Proton-exchange membrane (PEM) electrolysis is the technology we pursued for this design given its suitability for serving our high production goals, prevalence at commercial scale, and existence of reliable modeling techniques to gather process data. PEM electrolysis strikes a good balance between the benefits and drawbacks of the previous discussed technologies. It offers one of the highest gas purities of all the technologies (>99.999%) while maintaining high current densities (1-2 A/cm^2) for increased hydrogen production, both of which are critical for our design (Xu et al., 2022). PEM electrolyzers are also used by leaders in the industry such as Siemens in Germany and Nel in Norway, demonstrating the technology's commercial viability (Kumar and Lim, 2022). The only notable drawback of PEM electrolysis is its high cost, but we hope through our recommended design and economic analysis to illustrate the economic viability of this technology.

2.3.2 PEM Theory

Electrolysis can be described by the reactions that occur at the anode and cathode, known as half-reactions, that oxidize or reduce materials, respectively The relevant half-cell and full-cell reactions for the water electrolysis process are shown below:

$$H_2O \rightarrow 2H^+ + \tfrac{1}{2}O_2 + 2e^- \qquad (2\text{-}3\text{-}2\text{-}01)$$

$$2H^+ + 2e^- \rightarrow H_2 \qquad (2\text{-}3\text{-}2\text{-}02)$$

$$H_2O \rightarrow H_2 + \tfrac{1}{2}O_2 \qquad (2\text{-}3\text{-}2\text{-}03)$$

Equation 2-3-2-01 is the oxidation half-reaction occurring in the anode, equation 2-3-2-02 is the reduction half-reaction occurring in the cathode, and equation 2-3-2-03 is the

overall reaction. This third equation is the fundamental underpinning of this entire design: by supplying an external electromotive force, water can be split into the target hydrogen gas and a separate oxygen gas stream.

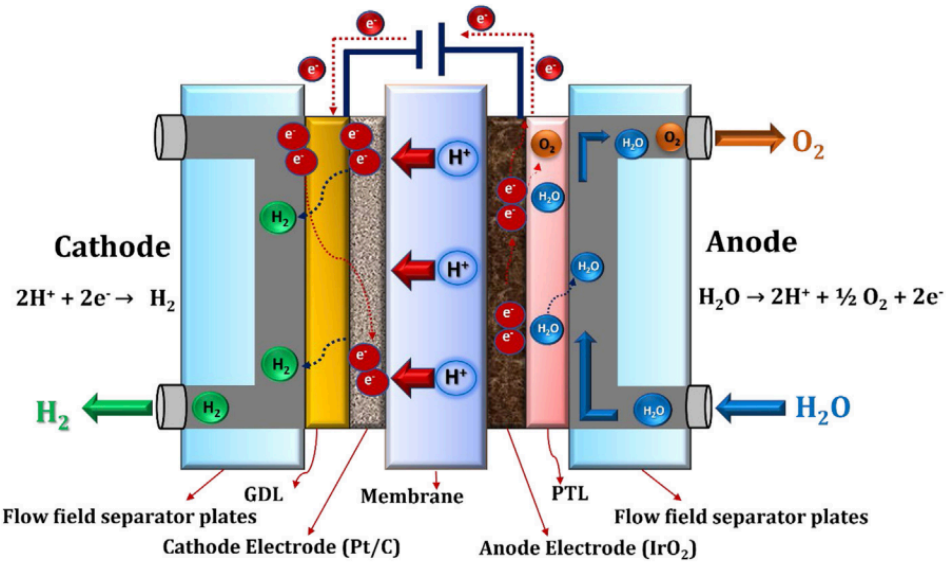

Figure 2-3-2-01: Schematic image of a PEM electrolyzer (Kumar and Lim, 2022).

Figure 2-3-2-01 shows a schematic representation of the PEM electrolyzer functionality. Water is split at the anode as indicated by the oxygen evolution reaction (Equation 2-3-2-01). The generated protons travel from the anode to the cathode through the membrane, at which point they gain electrons and evolve into hydrogen gas (Equation 2-3-2-02). This transport of the protons through a selective membrane is what makes PEM electrolysis different from other electrolysis types.

$$E^{0}_{rev} = \frac{\Delta G^{0}_{R}}{nF} \qquad (2\text{-}3\text{-}2\text{-}04)$$

$$V = E_{cell} + V_{Act,c} + V_{Act,a} + iR_{cell} \qquad (2\text{-}3\text{-}2\text{-}05)$$

$$E_{cell} = E^{0}_{rev} + \frac{RT}{2F}\left[ln\left(\frac{P_{H2}P_{O2}^{1/2}}{P_{H2O}}\right)\right] \quad (2\text{-}3\text{-}2\text{-}06)$$

$$V_{Act} = \frac{RT_a}{\alpha_a F} arcsinh\left(\frac{i}{2i_{0,a}}\right) + \frac{RT_c}{\alpha_c F} arcsinh\left(\frac{i}{2i_{0,c}}\right) \quad (2\text{-}3\text{-}2\text{-}07)$$

Equations 2-3-2-04 through 2-3-2-07 outline the foundational electrokinetics equations behind water electrolysis theory and our model. Equation 2-3-2-04 is the reversible cell potential difference between the anode and cathode. The water electrolysis reaction is not spontaneous at standard state (ΔG^0 = 236.483 kJ/mol, which is greater than 0, hence the non-spontaneity), so this reversible cell potential represents the minimum electrical work needed to drive the splitting reaction assuming thermal criteria are met. E^0_{rev} is 1.229 V for this reaction (Falcão and Pinto, 2020).

This potential is only valid at standard temperature and pressure, and because it is derived assuming no loss in the system, it represents the *minimum* potential required. In reality, there are activation losses, ohmic losses, and mass transport losses that necessitate an overpotential to drive the cell. Equation 2-3-2-05 represents these considerations. E_{cell} is the open circuit voltage, $V_{Act,c}$ and $V_{Act,a}$ are the activation overpotentials at the cathode and anode, respectively, i is the current density, and R_{cell} is the electrolyzer cell resistance. The literature on PEM modeling does not generally consider mass transport losses since those are only relevant at high current densities not typical for PEM electrolyzers (Falcão & Pinto, 2020).

Equation 2-3-2-06 is a form of the Nernst equation used to calculate the open circuit voltage mentioned in Equation 2-3-2-05. It relates the reversible cell potential discussed earlier with temperature and partial pressure of the outlet gasses at operating conditions to get the open circuit voltage. Equation 2-3-2-07 is the Butler-Volmer equation which relates exchange current

densities at the anode and cathode ($i_{0,a}$ and $i_{0,c}$) and the charge transfer coefficients at the anode and cathode (a_a and a_c) to the activation overpotential required at the electrodes to initiate the oxygen and hydrogen evolution reactions.

The goal of modeling is to use these kinetic equations to map current density (i) with final cell potential (V), in a relationship known as the polarization curve. From there, we can select an appropriate operating potential and calculate gas production.

2.3.3 Recommended PEM construction material choices from literature

One of the key design choices needed in our model was material of the electrolyzer components because that directly affects parameters such as conductivity and proton diffusion. Given a lack of ability to accurately test/simulate different materials, we reviewed the current literature and industrial recommendations for material design choices. The research on PEM electrolysis appears to be fairly consistent with regard to electrode and membrane choice, which is presented below.

2.3.3.1 Electrode material

Each of the half-reactions needs a suitable electrode material to catalyze the reaction. Literature recommends an iridium-oxide electrode for the anode and a platinum electrode for the cathode, both because of fast electrokinetics (Zhao et al., 2015). The exchange current density of platinum on carbon support is 0.2 A/cm^2 and the exchange current density of iridium oxide on carbon support is 0.05 A/cm^2. Smolinka et al. do note that ruthenium oxide has demonstrated better kinetics when used as the anode, but it is not suggested for industrial-scale applications because of its instability.

2.3.3.2 Membrane material

The membrane is the material in the middle of the membrane electrode assembly (MEA) and is responsible for facilitating the diffusion of the protons that are generated in the oxidation reaction from the anode to the cathode, where the protons are reduced and combined to form the target hydrogen gas (oxidation half-reaction shown in Equation 2-3-2-01 above). Literature suggests that the sulfonated tetrafluoroethylene-based fluoropolymer–copolymer, known as *Nafion*, is the industry standard for membrane choice in PEM electrolyzers. Nafion has a relatively high proton conductivity of 0.1 S/cm due to its sulfonic acid side chains and does not easily degrade, making it an ideal membrane choice (Kumar et al., 2018). This membrane has a lifetime of around 5 years (Office of Energy Efficiency and Renewable Energy, n.d.).

2.3.4 Modeling

We used a Simulink/MATLAB R2023b model adapted from a combination of the work presented by Liso et al. (2018) and Mo et al. (2016) for the PEM simulation.

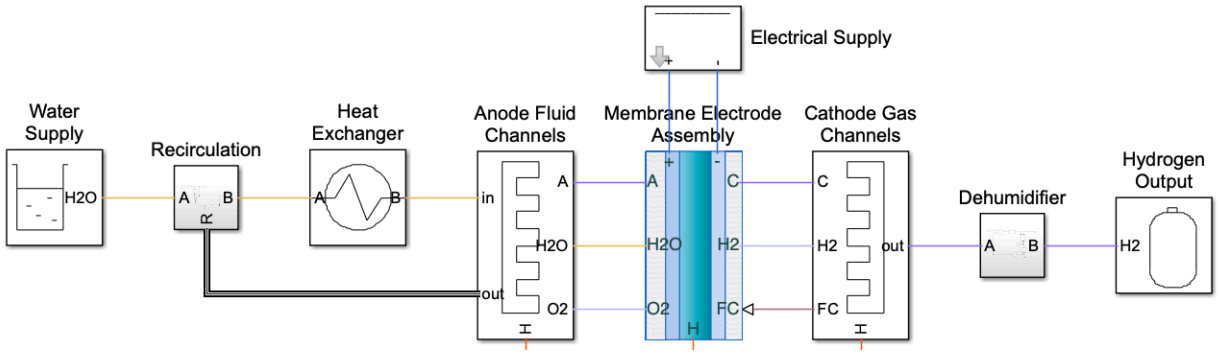

Figure 2-3-4-01. Simulink model of the PEM electrolyzer

Figure 2-3-4-01 shows the base model in Simulink with blocks for the membrane-electrode assembly (MEA), electrical supply, water input, and final hydrogen output.

We modified material properties, as discussed in section 2.3.3, from the baseline to reflect current industrial electrolyzer recommendations. Additionally, we tested and optimized three key process parameters: power source, stack size, and water temperature/pressure entering the electrolyzer. Given the initial design basis and assuming an 80% recovery of the hydrogen downstream, we calculated the target production rate of hydrogen gas for the electrolyzer to be 6500 kg/day.

2.3.4.1 Power source

Comparing the hydrogen production of a system connected to an intermittent solar power supply with a system connected to a constant power supply shows that the constant power supply produces more hydrogen (1870 kg H_2 per day on intermittent source versus 6500 kg H_2 per day on a constant source). Zhao et al. confirm this result by noting that electrolyzers are more efficient when minimizing variability in the power source (2015). This is a critical factor in our design, especially given the intermittent nature of renewable energy, which our plant must use to stay in line with decarbonization objectives. This is one of the other reasons for locating the plant in Sweden; power purchase agreements there have pledged a constant supply of on-shore wind energy, which we rely on to make the design work.

2.3.4.2 Cell sizing

A greater cell size increases the surface available for the hydrogen and oxygen evolution reactions but also requires more material for the electrodes, adding to capital cost. As expected, the modeling prefers increased cell sizing with regard to hydrogen production but also demands a greater power supply to maintain the necessary overpotential. Thus, cell sizing did not change

the final hydrogen production per kWh, which remained at roughly 0.026 kg H_2/kWh for all tested cell sizes (10 cm^2, 50 cm^2, 100 cm^2, 500 cm^2, 1000 cm^2, 1250 cm^2, 1500 cm^2).

2.3.4.3 Water temperature and pressure

Given that the river water can be near-freezing at some points in the year, one of the factors studied was the impact of inlet temperature on electrolyzer performance. Badgett et al. suggest that below 20˚C, electrolysis loses significant efficiency, so water temperatures between 20˚C and 90˚C were tested in increments of 10˚C to investigate its impact on electrolyzer performance. No significant differences were observed in hydrogen production over the interval (6480 kg H_2 per day at 20˚C and 6530 kg H_2 per day at 90˚C). Pressure had a similarly negligible effect on performance (for small changes in pressure beyond atmospheric level).

2.3.4.4 Operating values

A cell size of 1250 cm^2 was chosen based on the slightly higher hydrogen production per kWh (0.02604 kg H_2/kWh). 50 cells were assigned to a stack, which was a choice made based on commercial offerings of PEM electrolyzers (Kumar and Lim, 2022). For this sizing, a 100 kW constant power source was needed per stack to ensure the electrolysis takes place. Based on the polarization curve generated at these conditions and literature recommendations for PEM electrolyzers to avoid operation at high current densities (> 1.7 A/cm^2) to mitigate degradation and overheating, a current density of 0.98 A/cm^2 was chosen, which corresponds to an operating voltage of 1.63 V (Zhao et al., 2015). The reversible cell potential for water electrolysis is 1.229 V as noted in section 2.3.2, which puts the overpotential of each cell at 0.401 V. The current efficiency of the cell is 93.3%, meaning 6.7 kW of the 100 kW inlet is not put towards the

electrolysis reaction and instead dissipated as heat. Given that this dissipation is an order of magnitude smaller than the inlet power, cooling of the electrolyzer was not considered. Details of the final design specifications can be found in section 3.2.

2.4 Hydrogen Purification

2.4.1 Hydrogen Purity Exiting Electrolyzer

The purity of the hydrogen exiting the electrolyzer is determined by the temperature of the water in the electrolyzer, 25 °C. This determines the amount of dissolved air contaminants and water vapor present in the hydrogen stream leaving the electrolyzer. The amount of water vapor present in the hydrogen stream was calculated using the vapor pressure of water at 25°C and determined to be 3.13% using equation 2-4-1-01 below.

$$Water\ Vapor\ Fraction\ = \frac{Vapor\ Pressure}{Total\ Pressure} = \frac{3.171\ kPa}{101.325\ kPa} = 3.13\% \text{ (2-4-1-01)}$$

For dissolved air contaminants, Henry's Law was used to determine the solubility of a variety of gasses in water at 25°C; these gasses include nitrogen, oxygen, carbon dioxide, ozone, ammonia, argon, helium, neon, and helium. The Henry's Law equation and values used for each contaminant are summarized in equation 2-4-1-02 and Table 2-4-1-01, respectively. The Henry's Law constants were sourced from NIST and shown in Table 2-4-1-01. Additionally, the partial pressure of each gas contaminant was calculated using equation 2-4-1-03, which uses the contaminant volume percent, presented in Table 2-4-1-01, sourced from the NOAA (NOAA, 2023).

$$Solubility\ =\ K_h\ *\ Partial\ Pressure \text{ (2-4-1-02)}$$

$$Partial\ Pressure\ =\ P_{atmosphere}\ *\ Volume\ \% \text{ (2-4-1-03)}$$

Table 2-4-1-01 is shown below summarizing the K_h values, partial pressures, and subsequent calculations to determine the flow rate from electrolysis. The flow rate from electrolysis was determined from equation (2-4-1-04).

$$Flow\ Rate\ from\ Electrolysis\ =\ Reacted\ Water\ *\ Solubility\ *\ Molar\ Mass \quad (2\text{-}4\text{-}1\text{-}04)$$

Table 2-4-1-01. Henry's Law Calculations for Air Contaminants in Water

Gas Contaminant	K_h (mol/kg*bar)	Volume % in Air	Partial Pressure in Air (Pa)	Solubility (mol/kg)	Flow Rate from Electrolysis (kg/hr)
Nitrogen	0.0006	78	79,000	4.74e-4	3.17e-2
Carbon Dioxide	0.035	0.04	35.5	1.24e-5	1.3e-3
Oxygen	0.0013	21	21,300	2.77e-4	2.11e-2
Ozone	0.012	0.0467	47.3	5.68e-6	6.5e-4
Ammonia	27	0.00001	0.0101	2.74e-6	1.1e-4
Argon	0.0014	0.93	946	1.32e-5	1.26e-3
Neon	0.00045	0.001818	1.84	8.3e-9	3.98e-7
Helium	0.00038	0.000524	0.531	2e-9	1.98e-8

Furthermore, it is a possibility that the carbon dioxide may react within the electrolyzer to create carbon monoxide. Due to an unknown conversion of carbon dioxide, a conservative decision was made to conduct downstream purification processes under the assumption that all carbon dioxide was converted to carbon monoxide but still remained fully in the existing stream. The carbon monoxide flow rate was calculated using equation 2-4-1-05 below.

$$Flow\ Rate_{CO} = Flow\ Rate_{CO_2} * \frac{CO\ Molar\ Mass}{CO_2\ Molar\ Mass} \quad (2\text{-}4\text{-}1\text{-}05)$$

These impurity flow rates can now be added to the hydrogen flow rate exiting the electrolyzer and be used to determine the overall and water vapor flow rates exiting the electrolyzer; these are summarized in Table 2-4-1-02 below.

Table 2-4-1-02. Flow Rates for Hydrogen Stream Exiting Electrolysis

Component	**Flow Rate (kg/hr)**
Gas Impurities and Hydrogen	267.88
Water Vapor	77.11
Total Flow	345.00

2.4.2 Water Condenser

The condenser was placed immediately after the electrolyzer to remove the majority of the water vapor in the hydrogen stream. Because the water vapor is a relatively large percentage of the hydrogen stream, it is important to first remove a significant amount of the water vapor to allow for efficient separation of gas contaminants further downstream. Importantly, the water goes through a compressor before entering the condenser to increase the pressure to the required 900 kPA for the condenser.

When modeling the condenser unit, it was found that the heat requirement for the unit was much more dependent on the temperature at which the unit is run at than the pressure of the unit. A lower temperature will result in a higher water vapor removal, as will a higher pressure. However, as it is more energy efficient to increase the pressure of the condenser, it was decided that the pressure would be increased far more than the temperature would be decreased. The

pressure and temperature of this unit were determined based on a combination which yields a greater than 90% water removal when modeled in aspen.

The heat removal needed for this unit is provided by a cooling water jacket with cold river water running through it. Design specifications for the condenser were conducted on Aspen Plus v14, using the NRTL-RK method. Heat exchange area for the cooling jacket was also found using Aspen with a heat exchanger block representing the system.

2.4.3 Pressure Swing Adsorption (PSA)

The pressure swing adsorption system is needed to further purify the hydrogen gas by removing much of the remaining water vapor and reducing gas contaminants to acceptable levels. For the hydrogen separation, we have determined that 5A zeolite provides adequate adsorption of both water and gas contaminants, while minimizing hydrogen adsorption/loss. The temperature of the PSA is higher than that of the condenser, so an intermediate heat exchanger is needed (see 2.6.2.2)

The amount of 5A zeolite needed was determined by calculating the maximum amount of zeolite required to meet the required semiconductor-grade hydrogen specifications for each contaminant. The largest necessary amount of zeolite was, therefore, used in the column to meet all required specifications. Figures 2-4-3-01, A (Luberti, 2022), B (Talu, 1996), and C (Azhagapillai, 2022), were used to determine the amount of zeolite needed for each contaminant in our system.

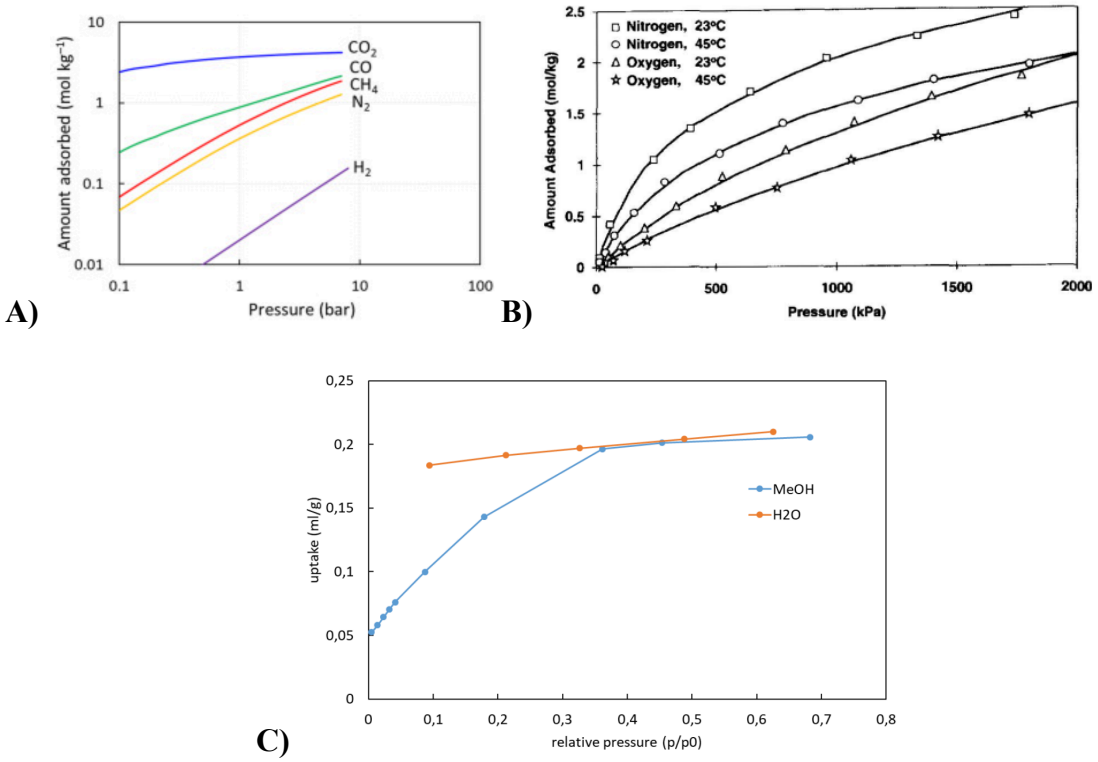

Figure 2-4-3-01 (A, B, C): A) Adsorption Isotherm for 5A Zeolite Gas Contaminants (Luberti, 2022); B) Adsorption Isotherms for Nitrogen and Oxygen on 5A Zeolite (Talu, 1996); C) Adsorption Isotherm for Water on 5A Zeolite (Azhagapillai, 2022)

The amount of zeolite needed was calculated using Equations 2-4-3-01, 2-4-3-02, and 2-4-3-03. Furthermore, after the amount of zeolite was determined, the amount of hydrogen exiting the PSA unit was determined using Equation 2-4-3-04.

$$Allowed\ Contaminant\ Flow\ Rate\ = \frac{Specified\ PPM}{10^6} * Hydrogen\ Flow\ Rate \quad (2\text{-}4\text{-}3\text{-}01)$$

$$Contaminant\ Adsorption\ Quantity\ = Allowed\ Contaminant\ Flow\ Rate\ - Entering\ Contaminant\ Flow\ Rate \quad (2\text{-}4\text{-}3\text{-}02)$$

$$Zeolite\ Needed\ =\ \frac{Contaminant\ Adsorption\ Quantity}{Adsorption\ Coefficient}$$ (2-4-3-03)

$$Hydrogen\ Exit\ Flow\ Rate\ =\ Entering\ Flow\ Rate\ -\ Adsorbed\ Quantity\ =$$

$$Entering\ Flow\ Rate\ -\ [Zeolite\ Quantity\ *\ Adsorption\ Coefficient]$$ (2-4-3-04)

Table 2-4-3-01 summarizes the specification PPM and adsorption coefficient from Figure 2-4-3-01; the table only includes values for contaminants which have required specifications.

Table 2-4-3-01. *Summary of Contaminant Specification PPM and Adsorption Coefficients*

Compound	**Specified PPM**	**Adsorption Coefficient**
Nitrogen	2	1.5
Carbon Dioxide	2	6
Carbon Monoxide	2	4
Oxygen	1	1.1
Water	3.5	8.889
Hydrogen	N/A	0.2

However, the zeolite bed will be fully saturated with contaminants after an hour of use; it is necessary to regenerate the zeolite bed after an hour of continued use. According to Talu et al., this can be accomplished by decreasing column pressure to lower gas contaminant adsorption capabilities and increasing temperature to remove adsorbed water molecules from the bed. A purge stream of the purified hydrogen can then be flowed through the column to remove the

contaminants. Based on our purity requirements, a purge stream containing 13% of the purified hydrogen stream should be used (Nikolic, 2007).

Because hydrogen has a high energy density of 33.6 kWh per kg hydrogen burned (RMI, 2019), burning the hydrogen used to purge the impurities in a furnace and converting it to electricity with a turbine allows the system to save money in electricity costs, assuming around 49% energy efficiency of the turbine (Power Engineering, n.d.), and that 100% of hydrogen gas is converted into steam (to be later vented to the atmosphere) following Equation 2-4-3-05 below.

$$H_2 + 1/2O_2 \rightarrow H_2O \quad (2\text{-}4\text{-}3\text{-}05)$$

2.4.4 Hydrogen Compression Process

This compression process is needed to meet the desired microelectronic grade hydrogen pressure of 70 MPa (700 bar). This process involves a multistage compressor sequence with intermediate heat exchangers to reduce the hydrogen temperature and improve compressor efficiency.

2.4.4.1 Compressors

To achieve the necessary compression, three stages will be needed to keep a reasonable compression ratio between 3 and 5. Furthermore, for more efficient compression, the hydrogen needs to be cooled down using a heat exchanger (see 2.4.4.2 for more). The compressors were modeled in Aspen Plus v14 as polytropic compressors using the American Society of Mechanical Engineers (ASME) method. It was assumed that no partial condensation of gas occurred in the interstage cooling.

2.4.4.2 Heat Exchangers

The heat exchanger units in between the compressor stages are needed to cool the compressed stream temperature and allow for more efficient hydrogen compression. The cooling stream for these heat exchangers is sourced from the Torne river water itself at 0°C. The exit temperature of this cooling water is 98°C for the first heat exchanger, 96°C for the second heat exchanger, and 99°C for the third heat exchanger. To minimize pumping costs, it is necessary to determine the minimum amount of water required to cool the hydrogen stream to 25°C. Additionally, as the hot water from the first condenser is being supplied to a previous heat exchanger to heat up the hydrogen stream exiting the condenser (see 2.6.2.2), the flowrate must be chosen to accommodate both needs.

This heat exchanger was modeled in Aspen Plus v14 as a countercurrent heat exchanger to obtain values for stream outlet temperatures, total heat transferred, and heat exchange area. The modeling equations used by Aspen are shown below in equations 2-4-4-2-01, 2-4-4-2-02, and 2-4-4-2-03.

$$Q = M * C_p * \Delta T \quad \text{(2-4-4-2-01)}$$

$$Q = U * A * \Delta T_{lm} \quad \text{(2-4-4-2-02)}$$

$$\Delta T_{lm} = \frac{\Delta T_{end\ 1} - \Delta T_{end\ 2}}{ln(\frac{\Delta T_{end\ 1}}{\Delta T_{end\ 2}})} \quad \text{(2-4-4-2-03)}$$

2.4.4.3 Bottling

The number of bottles needed will be based on a 250 L bottle and a hydrogen gas density at 25°C and 700 bar using the Redlich-Kwong Equation of state. Equation 2-4-4-3-01 will be used to calculate the number of bottles needed. The density was found to be 0.03987 kg/L using

Aspen properties. Additionally, Austenitic Stainless steel bottles will be used due to their resistance to hydrogen attack.

$$Number\ of\ Bottles\ per\ Year = \frac{Gas\ \ produced\ per\ year}{Density * 250} \qquad (2\text{-}4\text{-}4\text{-}3\text{-}01)$$

2.5 Oxygen Purification

2.5.1 Oxygen Purity Exiting Electrolyzer

The purity of the oxygen gas leaving the electrolyzer is determined by the temperature of the water in the electrolyzer, 25 °C. This determines the amount of dissolved air contaminants and water vapor present in the hydrogen stream leaving the electrolyzer. The amount of water vapor present in the oxygen stream was calculated by using the vapor pressure of water at 25°C, resulting in a water vapor fraction of 3.13% by using Equation 2-4-1-01.

For dissolved air contaminants, it was difficult to determine what amounts leave with the hydrogen versus the oxygen stream. For modeling purposes, a conservative assumption was made: all of the dissolved air contaminants exit with the oxygen stream. Thus, the contaminant calculations for oxygen are the same as hydrogen. So, again, Henry's Law was used to determine the solubility of air gasses in water at 25°C; these contaminant gasses include nitrogen, carbon dioxide, ozone, ammonia, argon, helium, neon, and helium. The Henry's Law equation and values used for each contaminant are summarized in equation 2-4-1-02 and Table 2-5-1-01, respectively. The constants used in Henry's Law were sourced from NIST and are shown in Table 2-5-1-01. The partial pressure of each gas contaminant was calculated using equation (2-4-1-03), which uses the contaminant volume percent, presented in Table 2-5-1-01, sourced from the NOAA (NOAA, 2023).

A table is shown below summarizing the K_h values, partial pressures, and subsequent calculations to determine the flow rate from electrolysis.

Table 2-5-1-01. Henry's Law Calculations for Air Contaminants in Water in Oxygen Stream

Gas Contaminant	K_h (mol/kg*bar)	Volume % in Air	Partial Pressure in Air (Pa)	Solubility (mol/kg)	Flow Rate from Electrolysis (kg/hr)
Nitrogen	0.0006	78	79,000	4.74e-4	1.59e-2
Carbon Dioxide	0.035	0.04	35.5	1.24e-5	6.55e-4
Oxygen	0.0013	21	21,300	2.77e-4	1.06e-2
Ozone	0.012	0.0467	47.3	5.68e-6	3.29e-4
Ammonia	27	0.00001	0.0101	2.74e-6	5.58e-5
Argon	0.0014	0.93	946	1.32e-5	6.36e-4
Neon	0.00045	0.001818	1.84	8.3e-9	2.0e-7
Helium	0.00038	0.000524	0.531	2e-9	9.68e-9

Unlike the scenario with hydrogen, because the oxygen is exiting in the anode, we expect that any carbon monoxide will be oxidized and reacted into carbon dioxide. Therefore, we assume that there will be no carbon monoxide remaining in the stream as an impurity.

The flow rates of the impurities can now be added to the oxygen flow rate exiting the electrolyzer and be used to determine the overall and water vapor flow rates exiting the electrolyzer which is summarized in Table 2-5-1-02 below.

Table 2-5-1-02. Flow Rates for Oxygen Stream Exiting Electrolysis

Component	Flow Rate (kg/hr)
Gas Impurities and Hydrogen	2132.12
Water Vapor	38.75
Total Flow	2170.86

2.5.2 Water Condenser

The condenser was placed immediately after the electrolyzer to remove the majority of the water vapor in the oxygen stream. Because the water vapor is a relatively large percentage of the oxygen stream, it is important to first remove a significant amount of the water vapor to allow for efficient separation of gas contaminants further downstream. Importantly, the water goes through a compressor before entering the condenser to increase the pressure to 608 kPa.

Similar to the condenser unit in the hydrogen purification process, it was found that the heat requirement for the unit was much more dependent on the temperature at which the unit is run at than the pressure of the unit. A lower temperature will result in a higher water vapor removal, as will a higher pressure. However, as it is more energy efficient to increase the pressure of the condenser, it was decided that the pressure would be increased more than the temperature would be decreased. A cooling water jacket with cold river water running through it is used to remove heat from this condensing unit. The design specifications for the condenser were conducted on Aspen Plus v14, using the NRTL-RK method. Heat exchange area for the cooling jacket was found using Aspen with a heat exchanger block representing the system.

2.5.3 Pressure Swing Adsorption (PSA)

The pressure swing adsorption system is needed to further purify the oxygen gas by removing much of the remaining water vapor and reducing gas contaminants to acceptable levels. For the oxygen separation, we have determined that 13X zeolite provides adequate adsorption of both water and gas contaminants, while minimizing oxygen adsorption/loss.

The amount of 13X zeolite needed was determined by calculating the maximum amount of zeolite required to meet the required research-grade oxygen specifications for each contaminant. The largest necessary amount of zeolite was, therefore, used in the column to meet all required specifications.

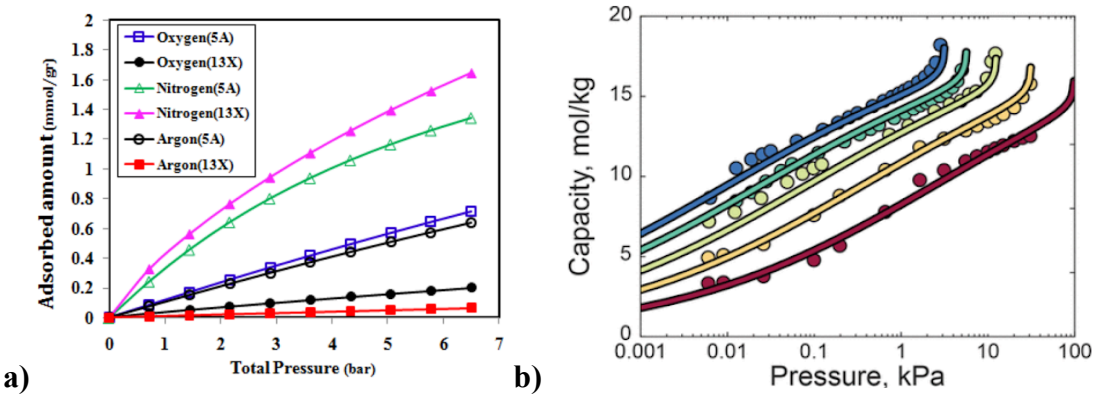

Figure 2-5-3-01 (a, b): a) Adsorption Isotherm for 13X Zeolite Gas Contaminants (Javadi, n.d.) ; b) Adsorption Isotherms for Water on 13X Zeolite (Son et al., 2019)

The amount of zeolite needed was calculated using equations 2-4-3-01, 2-4-3-02, and 2-4-3-03. Since water was the greatest contaminant in the oxygen stream, figure 2-5-3-01 (b) was used to determine the amount of zeolite needed at 20°C to meet the specifications for research grade oxygen. The graph shows the adsorption data for water at different temperatures: the dark blue represents water at 20°C, the turquoise line is water at 40°C, the light green is water at 60°C, the yellow is water at 80°C, and the red is water at 100°C. After determining that, figure

2-5-3-01 (a) was used to determine how much nitrogen and oxygen were removed with the amount of zeolite found that was needed to remove the water. After the amount of zeolite was determined, the amount of oxygen exiting the PSA unit was found using equation 2-4-3-04. Table 2-5-3-01 summarizes the specification PPM and adsorption coefficients from Figure 2-5-3-01; the table only includes values for contaminants which have required specifications.

Table 2-5-3-01. Summary of Contaminant Specification PPM and Adsorption Coefficients

Compound	Specified PPM	Adsorption Coefficient
Nitrogen	5	1.6
Water	0.5	16
Oxygen	N/A	0.6

The 15 kg of zeolite will be fully saturated with contaminants after an hour of use, so it is necessary to regenerate the zeolite bed after an hour for continued use. To properly regenerate the bed, the column should be purged with a portion of the purified oxygen stream at a vacuum gauge pressure of 0 kPa and a temperature of 400°C (Talu et al., 1996). The decreased pressure creates lower adsorption capability for the gas contaminants and the increased temperature removes the adsorbed water molecules from the bed. The purge oxygen stream will be used to sweep desorbed gas contaminants off of the zeolite, composed of 10% (volume basis) of total oxygen produced (Nikolic, 2007).

Consequently, the entire regeneration process will take roughly two hours: 37 minutes to heat up the purge stream and column from 32°C to 400°C, 45 minutes to purge at 400°C, and 37 minutes to cool down the column and purge stream. Therefore, two additional columns are

needed to achieve constant oxygen output during the regeneration process. The purged impure oxygen stream can be released to the atmosphere. Additionally, similar to hydrogen design, an extra adsorption column was added to the design to make a total of 4 columns; this was done to extend the longevity of all the columns and provide back-up if maintenance is needed on any of the other columns.

This PSA purification process ultimately produces an oxygen stream of 99.999904% oxygen, 0.405 ppm N_2, 0.01 ppm water, and 0.01 ppm CO_2 + CO with an overall oxygen recovery of 89% and a flow rate of 1917 kg/hr.

2.5.4 Oxygen Compression Process

This compression process is needed to meet the desired research grade oxygen pressure of 15200 kPa (2200 psi) (MESA Gas., n.d.). This process involves a multistage compressor sequence with intermediate heat exchangers to reduce the oxygen temperature and improve compressor efficiency.

2.5.4.1 Compressors

The purified oxygen stream exiting the PSA unit is at 20°C and 600 kPa. In order to bring this stream to 15200 kPa with a reasonable compressor ratio (3-5), it was found that 3 compressor units are needed with each compressor having a ratio of 2.94. This was modeled using the ‘mcompr’ function in the Aspen Plus v14 software where the compressors had an average power requirement of 241.7 kW, and the heat exchangers had an average power requirement of 227 kW.

2.5.4.2 Heat Exchangers

The heat exchanger units in between the compressor stages are needed to cool the compressed stream temperature and allow for more efficient hydrogen compression. The cooling stream for these heat exchangers is sourced from the Torne river water itself at 0°C. To minimize pumping costs, it is necessary to determine the minimum amount of water required to cool the oxygen stream to 25°C.

2.5.4.3 Bottling

The number of bottles needed will be based on a 250 L bottle and the oxygen gas density at 25°C and 15200 kPa using the Redlich-Kwong Equation of state. Equation (2-4-4-3-01) was used to calculate the number of bottles needed. The density was found to be 0.204 kg/L using Aspen properties. Additionally, carbon steel bottles will be used to bottle as there are no adverse reactions that should occur.

2.6 Ancillary Equipment

2.6.1 Pumps

Pumps were calculated using the equation 2-6-1-01 below, where P represents the hydraulic power requirement of the pump (in Watts), Q represents the volumetric flow rate (in m^3/s), and Δp represents the differential pressure (in Pa).

$$P = Q\Delta p \qquad (2\text{-}6\text{-}1\text{-}01)$$

Frictional loss in pipe was set to a conservative 50.66 kPa, and an additional 50.66 kPa was allocated for frictional loss due to the control valve, given that these are centrifugal pumps.

Furthermore, certain pumps (if applicable) were given an additional 50.66 kPa for loss through a heat exchanger and a gravity head, as calculated using the following equation

$$H_G = \rho g h \qquad (2\text{-}6\text{-}1\text{-}02)$$

H_G is the gravity head, ρ is the density of the fluid, g is the gravitational constant, and h is the height change traversed by the fluid.

2.6.2 Heat Exchangers

The final design has two heat exchangers, excluding those which are a part of the oxygen and hydrogen purification processes.

2.6.2.1 Purified Water Heat Exchanger

This heat exchanger plays the role of increasing the purified, river water temperature to 25°C. This is needed to optimize the electrolysis process, as well as allowing dissolved gasses to escape, making downstream separation easier. The water from the compression process is briefly split to supply the hydrogen purification heat exchanger (see 2.6.2.2). This water is then combined with the rest of the hydrogen compression water to be supplied to this water purification heat exchanger. The heated purified water is then briefly exposed to an air space to allow any previously dissolved gasses to exit the system.

This heat exchanger is modeled using the same methods as the previous heat exchangers. They are modeled in Aspen Plus v14 as a countercurrent heat exchanger to obtain values for stream outlet temperatures, total heat transferred, and heat exchange area. The modeling

equations used by Aspen are the previously shown equations 2-4-4-2-01, 2-4-4-2-02, and 2-4-4-2-03.

2.6.2.2 Hydrogen Purification Heat Exchanger

This heat exchanger is needed to increase the temperature of the hydrogen stream exiting the condenser to perform the PSA at the proper temperature. As mentioned in 2.6.2.1, a hot water stream from the compression process will be used to provide the heat needed for this exchange and will then be supplied to the water purification heat exchanger to further utilize any remaining heat. The split stream of heated water from the hydrogen multistage compression process enters this heat exchanger with a flowrate of 2000 kg/hr and a temperature of 98 °C; it exits at a temperature of 93°C. It heats up the hydrogen exiting the condenser from a temperature of 20°C to 32°C.

As with the other heat exchangers, this was modeled using Aspen Plus v14 as a countercurrent heat exchanger to obtain values for stream outlet temperatures, total heat transferred, and heat exchange area. The modeling equations used by Aspen are the previously shown equations 2-4-4-2-01, 2-4-4-2-02, and 2-4-4-2-03.

3. Recommended Design

3.1 Water Pretreatment Process

The figure below shows the overall process flow diagram (PFD) for the water pretreatment process.

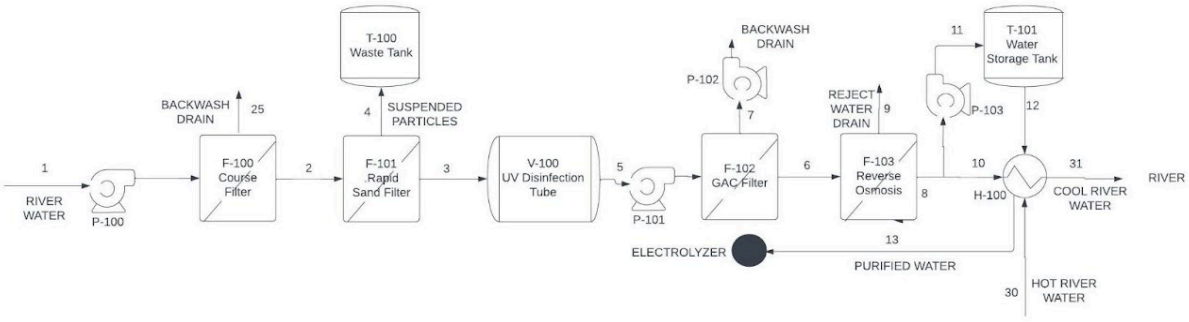

Figure 3-1-01: Overall PFD for Water Pretreatment Process

Additionally, relevant streams within this process are shown below.

Table 3-1-01. Water Purification Stream Table

Stream Number	Flowrate (kg/hr)		Main Component
	Normal Operation	GAC Backwashing	
1	8994.80	13258.56	Water
2	7195.82	10606.85	Water
3	7195.82	10606.85	Water
4	0.037	0.055	Suspended Particles
5	7195.82	10606.85	Water
6	7195.82	7195.82	Water
7	n/a	3411	Water
8	2374.62	n/a	Water
9	4821.20	n/a	Water
10	2137.16	n/a	Water
11	237.46	n/a	Water
12	237.46	n/a	Water
13	2374.62	n/a	Water
25	1798.96	n/a	Water
30	6000	n/a	Water
31	6000	n/a	Water

3.1.1 Coarse Mesh Screen (P-100, F-100)

As mentioned earlier, we will be using the RF100 Duplex Pump Self-Cleaning Filter seen in Figure 2-2-1-01. This pump is equipped with a 250 μm filter. As seen in Table 3-1-01, 8994.8 kg/hr of water will enter F-100 from stream 1 during normal operations and 13,258 kg/hr during GAC backwashing. The continuous backwashing system uses 25% of the pump's inlet water (1798.96 kg/hr during normal operations and 2651.71 kg/hr during GAC backwashing) to drive the internal backwashing, cleaning the whole screen every 0.5 seconds. The continuous backwash stream will be disposed of directly back into the river in stream 25 via a drain line.

The filter's mesh is a nylon material that will be cleaned with water and detergent during summer shutdown in July and each filter will be replaced during end-of-year shutdown in December.

3.1.2 Rapid Sand Filter (F-101)

After the fine mesh filter, the water enters F-101 in stream 2 at 7,195 kg/hr during normal operations and 10,606 kg/hr during GAC backwashing. The Parkson DynaSand® Filter (Parkson, n.d.) uses the No. 20 Silica Sand (diameters between 0.45 mm and 0.55 mm) to capture impurities as small as 20 μm (Miller, 2024) and it removes 99% of SPM impurities. This filter will have a fiberglass-reinforced plastic (FRP) shell. The filter has a bed depth of 2.032 m (80 in) and a cross-sectional area of 0.73 m^2.

The Parkson DynaSand® Filter also has a continuous backwashing system that uses air to pump a 1:1 slurry of the removed suspended particles and water in stream 4 out a drain line into a waste tank (T-100) at 0.037 kg/hr under normal operations and 0.055 kg/hr during GAC

backwashing. The 20 Silica Sand is replaced every two to three years, and an evaluation of its conditions will be performed during the end-of-year shutdown in December.

3.1.3 Waste Tank (T-100)

The SPM waste filtered out of the water will be collected in the waste tank T-100. This is a 50 L carbon steel tank that will be emptied on the 28th of each month.

3.1.4 UV Disinfection (V-100)

After the rapid sand filter, the water passes through V-100 at 7,195 kg/hr during normal operations and 10606 kg/hr during GAC backwashing. The Polaris Scientific UVA-60B product removes up to 99.99% of these live contaminants and is equipped with 5 LED lamps that emit a wavelength of 254 nm. The 304 stainless steel tube has dimensions of 13.9 cm x 93.8 cm (5.5 x 36.93 in). The target residence time is ~3.8 sec. The dead cell-debris will then be filtered out by either the GAC filter or the RO system. The UV disinfection tube lamps will be replaced during the end-of-year shutdown in December.

3.1.5 GAC Filter (F-102)

After UV disinfection, the water is sent through a granular activated carbon (GAC) filter (F-102). The Eagle Redox Alloy® (ERA) (Crystal Quest Water Filters, n.d.) media consists of high purity copper-zinc granules. Again, the water enters at 7,195 kg/hr water under normal operations and 10,606 kg/hr during backwashing. The GAC filter will have a cross-sectional area of 0.22 m^2 and will be backwashed every three days for 20 minutes.

We will install two GAC filters in parallel where only one will be operational at a time. Every three days, the GAC filters will be alternated in order to perform backwashing. During the transition, the flow rate will temporarily increase from 7,195 kg/hr to 10,606 kg/hr of water in order to maintain a constant volume of water flowing to the RO unit while also accommodating the backwash process. Once backwashing is complete, the flow rate will decrease back to 7,195 kg/hr water. The backwashed water will exit out of a drain line in stream 7 and will be pumped and released to the nearby ocean. The GAC filter membranes will be replaced every year (Fresh Water Systems, n.d.) during the end-of-year shutdown in December.

3.1.6 Reverse Osmosis and Water Storage Tank (F-103, T-101)

The RO unit F-103 has an efficiency of 33%. Our process requires an input flow rate of 7195 kg/hr of water (stream 6) into the RO system at 4.06 atm. We will be installing four RO units in parallel that each have a maximum capacity of 6,548 kg/hr of water and 14 membranes. Two RO units will be operational at a time. On the 28th of each month (also when the GAC filters are swapped), the RO units will be swapped for cleaning and maintenance. With proper maintenance, these RO units are expected to last 4 years (US Water Systems, 2023). The reject water will be disposed of directly into the river through stream 9.

The water storage tank is designed to hold 4 hours' worth of purified water in case there are any unexpected issues with the water-pretreatment system. During the start-up process, the water storage tank will be filled with 9.53 m^3 of purified water. This will be held in a 10,000 liter carbon steel tank. Once this target is hit, the valve on stream 12 and stream 10 will open and the process will run continuously, feeding the heat exchanger a steady 2374 kg/hr of water.

3.2 Proton-Exchange Membrane (PEM) Electrolyzer Design

The overall process flow diagram (PFD) for the electrolysis system is shown below.

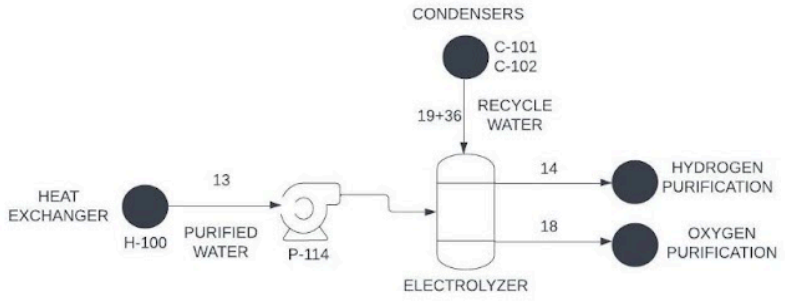

Figure 3-2-01: Overall PFD for PEM Electrolysis

The overall process flow diagram (PFD) for the electrolysis system is shown below.

Table 3-2-01: Stream Table for PEM Electrolysis

Stream Number	Flowrate (kg/hr)	Main Component
13	2374.62	Water
14	345.00	Hydrogen
18	2170.86	Oxygen
19	36.28	Water
36	70.74	Water

We recommend a proton-exchange membrane (PEM) electrolyzer (R-100) for the design because it is a proven technology that offers one of the more promising efficiencies, both in terms of hydrogen production and energy usage. There are several key design considerations for

the electrolyzer: membrane type, anode/cathode catalyst, inlet water temperature/pressure, cell sizing, and power source.

3.2.1 Electrolyzer material recommendations

For membrane type and electrode catalysts, we follow current industrial choices and literature recommendations. Our design uses Nafion for the membrane, iridium oxide for the anode, and platinum for the cathode. The membrane should be replaced every 5 years to maintain proton conductivity, and we assumed for our design that the electrodes last the lifetime of the plant (Zhao et al., 2015).

3.2.2 Water temperature and pressure recommendations

Inlet water temperature and pressure of streams 13, 19, and 36 will be set to 25˚C and 1 atm, respectively, given the minimal effect of these two parameters on hydrogen production. While a slightly higher temperature produces more hydrogen, we estimate that it is not worth the additional energy requirement for the heat exchanger, so the cells will also be operating at 25˚C. Keeping the pressure at atmospheric level also reduces the hydraulic power requirement of the pump.

3.2.3 Cell sizing recommendations

On a mole basis, 99.8% of inlet water gets converted into hydrogen gas on a single pass. This high conversion is expected given the extensive pretreatment done to eliminate any contaminants in the inlet water. We found a 1250 cm^2 cell size running on 100 kW had the best hydrogen production-to-power ratio. Each cell produces 0.026 kg hydrogen per kWh consumed.

50 cells were assigned to a stack, producing 52 kg H_2 per day. To reach the overall production goal with intentional overdesign to account for losses in the purification system, 125 stacks were chosen to bring the final daily production of hydrogen from the electrolyzer to 6500 kg per day.

3.2.4 Polarization curve

Figure 3-2-02 below shows the final polarization curve after modeling with the recommended design parameters.

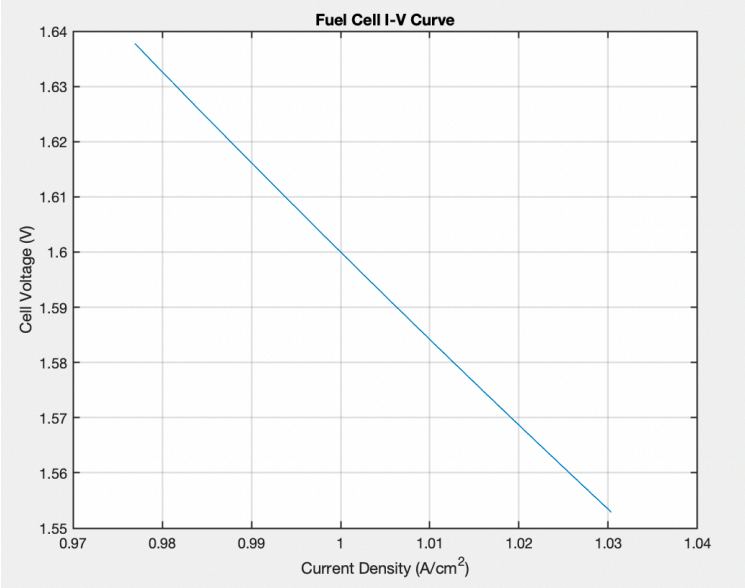

Figure 3-2-02. Polarization curve for the PEM electrolyzer at design specifications

The voltage versus current density curve is approximately linear (over a small range of voltages and current densities) due to the constant power supply. The voltage also decreases as current density increases, which is to be expected. Zhao et al. emphasize that PEM electrolyzers do not work well at high current densities (> 1.7 A/cm^2) because of degradation and overheating effects of large current densities, so a voltage corresponding to a relatively low current density

was chosen (2015). For this system, each cell will be operating at 1.63 volts and a current density of 0.98 A/cm^2.

3.2.5 Power consumption

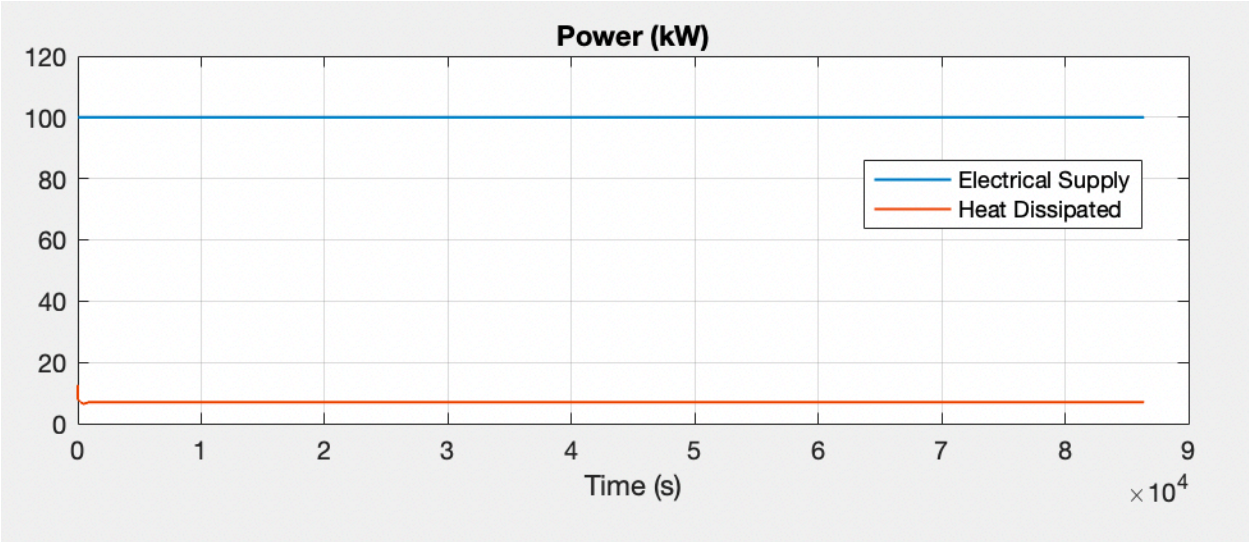

Figure 3-2-03. Power consumption and heat dissipation per stack of the PEM electrolyzer

A 100 kW constant power supply that will be connected to each of the 125 stacks in R-100. Due to cell losses discussed in section 2.3.2, some of the electrical work will not be put towards driving the reaction; instead, it will be dissipated as heat. Each stack will dissipate about 6.7 kW constantly, which is an order of magnitude less than the energy supply (Figure *3-2-03*). This heat also does not seem to significantly impact electrolyzer performance, so we do not require any cooling and regulation for the design.

3.2.6 Electrolyzer recommendation summary

Below is a table summarizing the final design recommendations for R-100.

Table 3-2-02. Electrolyzer design specifications chosen based on PEM modeling

Parameter	**Design Specification**
Number of stacks	125
Number of cells per stack	50
Cell area	1250 cm^2
Inlet water temperature (to electrolyzer)	25˚C
Inlet water pressure (to electrolyzer)	1 atm
Power supply (per stack)	100 kW
Voltage (per cell)	1.63 V
Current density (per cell)	0.98 A/cm^2
Membrane material	Nafion
Anode material	Iridium Oxide
Cathode material	Platinum

3.3 Hydrogen Separation

Figure 3-3-01 below depicts the overall process flow diagram (PFD) for the hydrogen separation process.

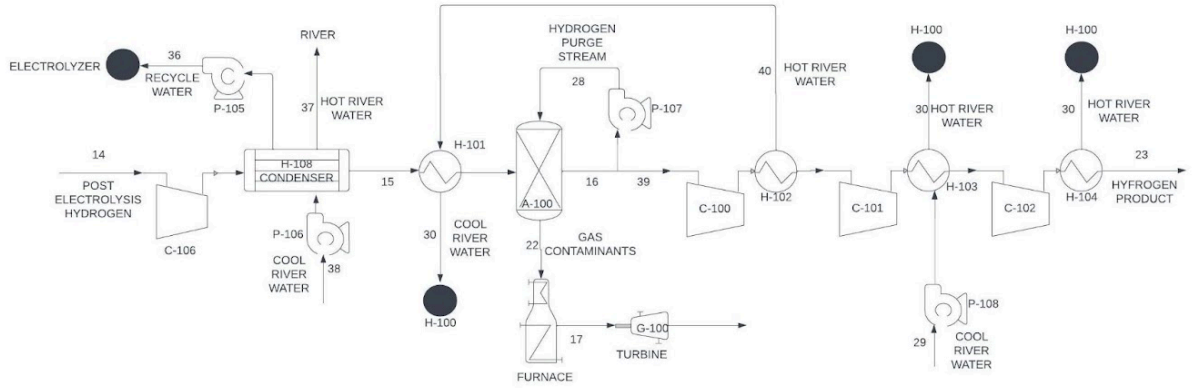

Figure 3-3-01: Overall PFD for Hydrogen Separation

Table 3-3-01 below depicts the stream table for all relevant streams within the hydrogen separation process.

Table 3-3-01. Hydrogen Separation Stream Table

Stream Number	Flowrate (kg/hr)	Temperature (℃)	Pressure (kPa)	Main Component
14	345	25	101.325	Hydrogen
15	274.26	20	900	Hydrogen
16	267.82	32	900	Hydrogen
17	181.06	760	900	Steam
22	20.63	32	900	Hydrogen + Impurities
23	233	25	70000	Hydrogen
28	17.41	32	900	Hydrogen
29	6000	0	101.325	Water
30	6000	95.78	101.325	Water
36	70.74	20	900	Water
37	5000	92.9	101.325	Water
38	5000	0	101.325	Water
39	233	32	900	Hydrogen
40	2000	98.1	101.325	Hydrogen

This hydrogen separation process is needed to meet product purity and certain gas specifications to sell to the microelectronics industry. To achieve this specification, a condenser and pressure swing adsorption (PSA) process are used to remove water and other gas impurities from the hydrogen stream exiting the electrolyzer.

3.3.1 Water Condenser (H-108, C-106)

The condenser has been designed to run at a temperature of 20°C and at 900 kPa. Before the water enters this condenser, it will go through a compressor (C-106) to increase the pressure to 900 kPa; this also increases the temperature to 430°C. 5000 kg/hr of cooling water (stream 38) from the river at a temperature of 0°C will be used to keep the condenser temperature at 20°C and remove the -508 kW heat duty; the cooling water exits at a temperature of 71.37°C. The area required for this heat exchange is 24.8 sq. meters. This resulted in 92% water removal and created an exit stream of 0.27% water vapor and 99.7% hydrogen.

3.3.2 Pressure Swing Adsorption (PSA) (A-100)

The column is set to operate at 32°C and 900 kPa, as this allows for a quality separation of hydrogen and contaminants than other pressures and temperatures (Luberti & Ahn, 2022). As the column is operating at 32°C and the stream exiting the condenser is at 20°C, it is necessary to increase the hydrogen stream temperature with a heat exchanger (See 3.5.2.2).

From these calculations, it was determined that roughly 40 kg of 5A zeolite are needed to achieve the required contaminant purity requirements, for one hour of flow. This resulted in a single pass hydrogen recovery of 99.994%.

This is not, however, the overall hydrogen recovery, as some of the hydrogen must be used in combination with a pressure swing, to regenerate and desorb the zeolite bed (stream 28). To properly regenerate the bed, the column must be purged with a portion of the purified hydrogen stream at a gauge vacuum pressure of 0 kPa and a temperature of 400°C (Talu, 1996). The purge hydrogen stream will be used to sweep desorbed gas contaminants off of the zeolite, composed of 13% (volume basis) of total hydrogen produced (Nikolic, 2007). This sweep stream will additionally result in an increase of the bed's temperature temperature from 32°C to 400°C at a rate of 10°C/min (Azhagapillai, 2022). This yields an 87% hydrogen recovery rate.

Consequently, the entire regeneration process will take roughly two hours: 37 minutes to heat up the purge stream and column from 32ºC to 400ºC, 45 minutes to purge at 400°C, and 37 minutes to cool down the column and purge stream. This requires two additional columns to achieve constant hydrogen output during the regeneration process. Importantly, the purge gas is collected over an hour but must be released over two hours. Therefore, a tank (not shown) should be used to hold the gas when collected. This makes the flowrate of stream 28 half of what it would be, otherwise.

The purged, impure hydrogen stream will be burned and reacted into steam. This steam (stream 17) will be burned in a furnace, then converted to electricity by propelling a stainless steel, axial gas turbine, providing an extra 274 kW of energy which will be supplemented towards the multistage hydrogen compression unit. Additionally, an extra (4th) adsorption column was added to the design to extend the longevity of all the columns and provide back-up if maintenance is needed on any of the other columns.

This PSA purification process ultimately produces a hydrogen stream of 99.9996% hydrogen, 0 ppm N_2, 0 ppm O_2, 0 ppm CO_2, 0 ppm CO, and 3.49 ppm water with a hydrogen recovery of 97% and a flow rate of 233 kg/hr.

3.3.3 Hydrogen Compression

3.3.3.1 Compressors (C-100, C-101, C-102)

The purified hydrogen exiting the PSA unit (stream 16 & 39) is at 32°C and 900 kPA. In order to bring this stream to 70 MPa, 3 compressor units are needed with a ratio of 4.267.

The first stage increases the stream pressure from 900 kPa to 3840 kPA; due to the compression, the temperature of the stream was increased to 270°C. This was then lowered to 25°C in a heat exchanger (see 3.3.3.2 Heat Exchangers). The stage had a power requirement of 225 kW. The second stage increased the stream pressure from 3840 kPA to 16.4 MPa, while increasing the temperature to 260°C. Again, the temperature was lowered to 25°C. This stage had a power requirement of 227 kW. Lastly, the third stage increased the stream pressure from 16.4 MPa to 70 MPa and increased the temperature to 270°C. This stage had a power requirement of 260 kW, yielding a total compressor power requirement of 712 kW. Again, a heat exchanger was used after this step to cool the hydrogen stream to 25°C.

3.3.3.2 Heat Exchangers (H-102, H-103, H-104)

It was determined that the minimum cooling water flow rate needed to cool the hot compressed hydrogen streams, while staying within the liquid phase is 6,000 kg/hr (stream 29). The supplied cooling river water has a temperature of 0°C. This yields a post heat exchanger temperature of 98°C for the first heat exchanger, 96°C for the second heat exchanger, and 99°C

for the third heat exchanger. The three heat exchangers had areas of 3.55 m^2, 3.52 m^2, and 3.63 m^2, respectively. It should be noted, however, that a yearly fluctuating river water temperature may require different cooling water flow rates throughout the year. However, given that this river is sourced from glacial melt, we do not believe the river water temperature will have large fluctuations and 6,000 kg/hr should be an adequate all-around cooling water flow rate.

3.3.3.3 Bottling

A quantity of 1,538,400 250 L bottles per year of Austenitic Stainless steel are needed for this bottling process.

3.4 Oxygen Separation

Figure 3-4-01 below depicts the overall process flow diagram (PFD) for the oxygen separation process.

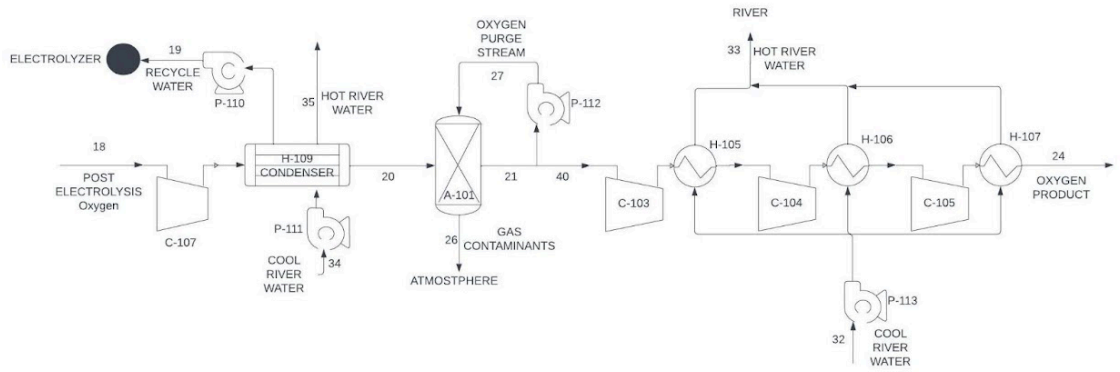

Figure 3-4-01: Overall PFD for Oxygen Separation

Table 3-4-01 below depicts the stream table for all relevant streams within the oxygen separation process.

Table 3-4-01. Oxygen Purification Stream Table

Stream Number	Flowrate (kg/hr)	Main Component
18	2170.86	Oxygen
19	36.28	Water
20	2134.58	Oxygen
21	2129.72	Oxygen
24	2129.72	Oxygen
26	215.4	Oxygen + Impurities
27	212.97	Oxygen
32	6000	Water
33	6000	Water
34	4000	Water
35	4000	Water

This oxygen separation process is necessary in order to meet product purity and certain gas specifications to sell to the research industry. A condenser and pressure swing adsorption (PSA) process are used to remove water along with other gas impurities from the oxygen stream exiting the electrolyzer.

3.4.1 Water Condenser (H-109, C-107)

The condenser has been designed to operate at a temperature of 20°C and at 608 kPa. Before the water enters this condenser, it will go through a compressor (C-107) to increase the pressure to 608 kPa; this also increases the temperature to °C. 4000 kg/hr of cooling water (stream 34) from the river at a temperature of 0°C will be used to keep the condenser temperature at 20°C and remove the -176.75 kW heat duty. The stream exits at a temperature of 40°C. The area required for this heat exchanger that maintains the condenser temperature is 3.56 sq. meters. This process allowed for 87.8% of the water to be removed from the oxygen stream, resulting in an exit stream of 0.39% water vapor and 99.6% oxygen.

3.4.2 Pressure Swing Adsorption (PSA) (A-101)

The column is operating at 20°C and 600 kPa, as this allows for optimal separation of oxygen gas from the contaminants in the stream. It was determined that roughly 15.3 kg of 13X zeolite are needed to achieve the required contaminant purity specifications. This resulted in a single pass oxygen recovery of 99.995%.

Since some of the oxygen is used in combination with a pressure swing to regenerate and desorb the zeolite bed, this is not the overall oxygen recovery. To properly regenerate the bed, the column must be purged with a portion of the purified oxygen stream at a gauge vacuum pressure of 0 kPa and a temperature of 400°C (Talu, 1996). The purge oxygen stream will be used to sweep desorbed gas contaminants off of the zeolite, composed of 10% (volume basis) of total oxygen produced (Nikolic, 2007). This sweep stream will additionally result in an increase of the bed's temperature temperature from 32°C to 400°C at a rate of 10°C/min (Azhagapillai, 2022).

This yields an 89.995% oxygen recovery rate. This purged oxygen stream will be vented to the atmosphere (stream 26).

The entire regeneration process will take about 2 hours to complete: 37 minutes to heat up the purge stream and column from 32°C to 400°C, 45 minutes to purge at 400°C, and 37 minutes to cool down the column and purge stream. As a result, this regeneration process requires two additional columns to achieve constant oxygen output during the regeneration process, with one extra for backup, totaling 4 PSA columns.

This PSA purification process ultimately produces an oxygen stream of 99.9999% O_2, 0.405 ppm N_2, 0.01 ppm CO_2, 0 ppm CO, and 0.001 ppm water with an oxygen recovery of 89% and a flow rate of 1917 kg/hr.

3.4.3 Oxygen Compression

3.4.3.1 Compressors (C-103, C-104, C-105)

The purified oxygen exiting the PSA unit is at 20°C and 600 kPA. In order to bring this stream to 15200 kPa with a reasonable compressor ratio (3-5), it was found that 3 compressor stages are needed with each compressor having a ratio of 2.94.

The first stage increases the stream pressure from 600 kPa to 1764 kPa; due to the compression, the temperature of the stream was increased to 172°C. This was then lowered to 25°C in a heat exchanger (H-105). The stage had a power requirement of 75.15 kW. The second stage increases the stream pressure from 1764 kPa to 5186 kPa; due to the compression, the temperature of the stream was increased to 179°C. Again, this was then lowered to 25°C in a heat exchanger (H-106). The stage had a power requirement of 76.13 kW. The third stage increases the stream pressure from 5186 kPa to 15247 kPa; due to the compression, the

temperature of the stream was increased to 177°C. This was then lowered to 25°C in a heat exchanger (H-107). The stage had a power requirement of 75.62 kW, yielding a total compressor power of 227 kW.

3.4.3.2 Heat Exchangers (H-105, H-106, H-107)

It was determined that the minimum cooling water flow rate needed to cool the hot compressed hydrogen streams, while staying within the liquid phase is 6,000 kg/hr (stream 32). The supplied cooling river water has a temperature of 0°C. This yields a post heat exchanger temperature of 33°C for the first heat exchanger, 35°C for the second heat exchanger, and 38°C for the third heat exchanger. The three heat exchangers had areas of 1.314 m^2, 1.398 m^2, and 1.538 m^2, respectively. It should be noted, however, that a yearly fluctuating river water temperature may require different cooling water flow rates throughout the year. However, given that this river is sourced from glacial melt, we do not believe the river water temperature will have large fluctuations and 6,000 kg/hr should be an adequate all-around cooling water flow rate.

3.4.3 Bottling

36,550 250 L bottles each year made of Carbon steel are needed for this bottling process.

3.5 Ancillary Equipment

3.5.1 Pumps

The final design has a total of 18 pumps operating at all times. For each unique stream location which requires a pump, one spare pump is allocated. There are 4 pumps for river water intake, which come attached to the fine mesh mechanical screen that serves as the first step of the

water pretreatment. Otherwise, there is only one pump for all other relevant locations. Table 3-5-1-01 below shows the differential pressure, volumetric flow rate, and hydraulic power for each pump in the process.

Table 3-5-1-01. Pump Summary

Equipment Name Stream	Differential Pressure (kPa)	Volumetric Flowrate (m^3/s)	Hydraulic Power (W)
P-100	411.38	0.0037	1520
P-101	755.88	0.0029	2230
P-102	445.83	0.00095	422
P-103	131.72	0.000066	8.67
P-105	658.61	0.00020	129
P-106	151.98	0.0014	211
P-107	1013.25	0.0059	6030
P-108	151.98	0.00167	253
P-110	658.61	0.000010	6.64
P-111	151.98	0.0011	167
P-112	709.28	0.0046	3230
P-113	151.98	0.00167	253
P-114	151.99	0.00066	100

Most pumps in the system will have water as the fluid, except for streams 14, 18, 27, and 28, which contain either oxygen or hydrogen gas that is produced from the electrolyzer and

coming out of pressure-swing adsorption. There are no additional material considerations for these fluids, so carbon steel centrifugal pumps with control valves were chosen for the design. These will operate at about 70% efficiency.

3.5.2 Heat Exchangers

This section details the design of the two remaining heat exchangers not associated with hydrogen and oxygen compression. A summary of all heat exchangers is shown in Table 3-5-2-01.

Table 3-5-2-01. Heat Exchanger Summary

Heat Exchanger	Cold Inlet Temperature (°C)	Cold Outlet Temperature (°C)	Hot Inlet Temperature (°C)	Hot Outlet Temperature (°C)	Heat Exchanger Area (m^2)
H-100	0	25	95.8	86.6	1.00
H-101	20	32	98	93	0.22
H-102	0	98	270	25	3.55
H-103	0	96	260	25	3.52
H-104	0	99	270	25	3.63
H-105	0	33	172	25	1.31
H-106	0	35	179	25	1.40
H-107	0	38	177	25	1.54
H-108	0	12	25	20	8.03
H-109	0	4.04	25	20	1.34

3.5.2.1 Water Purification Heat Exchanger (H-100)

Heated water from the hydrogen multistage compression process (stream 30) is sent through this heat exchanger to heat up cold, purified, river water at a temperature of 0°C to 25°C. The heated water enters the heat exchanger at a flow rate of 6000 kg/hr and a temperature of 95.8°C (after merging with the split stream supplied to the hydrogen heat exchanger, see 3.5.2.2); the stream exits the heat exchanger at a temperature of 86.6°C. Given these requirements, the heat exchanger uses a double pipe, carbon steel, shell and tube configuration with 1 square meter of heat transfer area.

3.5.2.2 Hydrogen Purification Heat Exchanger (H-101)

A split stream of heated water from the hydrogen multistage compression process (stream 40) is sent through this exchanger to heat up hydrogen exiting the condenser at a temperature of 20°C to 32°C for proper separation in the PSA unit. The heated water enters the heat exchanger at a flow rate of 2000 kg/hr and a temperature of 98°C; the stream exits the heat exchanger at a temperature of 93°C and mixes back with stream 30 to enter the water purification heat exchanger. Given these requirements, the heat exchanger uses a double pipe, carbon steel, shell and tube configuration with 0.22 square meters of heat transfer area.

3.6 Plant Operation Schedule

The following chart (Figure 3-6-01) shows the plan for our operational schedule. Out of the 8760 hours in the year, we will be operating for 8000 hours to hit the per annum hydrogen production design target. This equates to about 335 days of operation and 30 days of downtime. Green indicates regular operational hours, when the process has reached steady-state, and counts

towards the 335 days of operation. Grey indicates scheduled maintenance. There are two routine long-term maintenance blocks allotted in the year: one week at the end of the calendar year (December 25 - January 2 of the next year) and one week in the middle of the year (July 11 - July 19). This is where larger but expected maintenance projects such as electrolyzer membrane replacement, GAC/RO membrane replacement, and inlet mesh screen cleaning. Yellow indicates start-up and shutdown processes, which are scheduled for before and after maintenance weeks. Production during this time will not be at normal, steady-state capacity. Orange indicates alternation of GAC and RO units, which occurs once a month to ensure both filtrations are running at expected levels. Blue indicates unscheduled maintenance, reserved for unintended downtime where equipment needs to be serviced. There are nine days allotted for these shorter-term maintenance projects, which are currently set at the first of every month, but in reality they will occur as needed throughout the year. Otherwise, the normal operating schedule will follow.

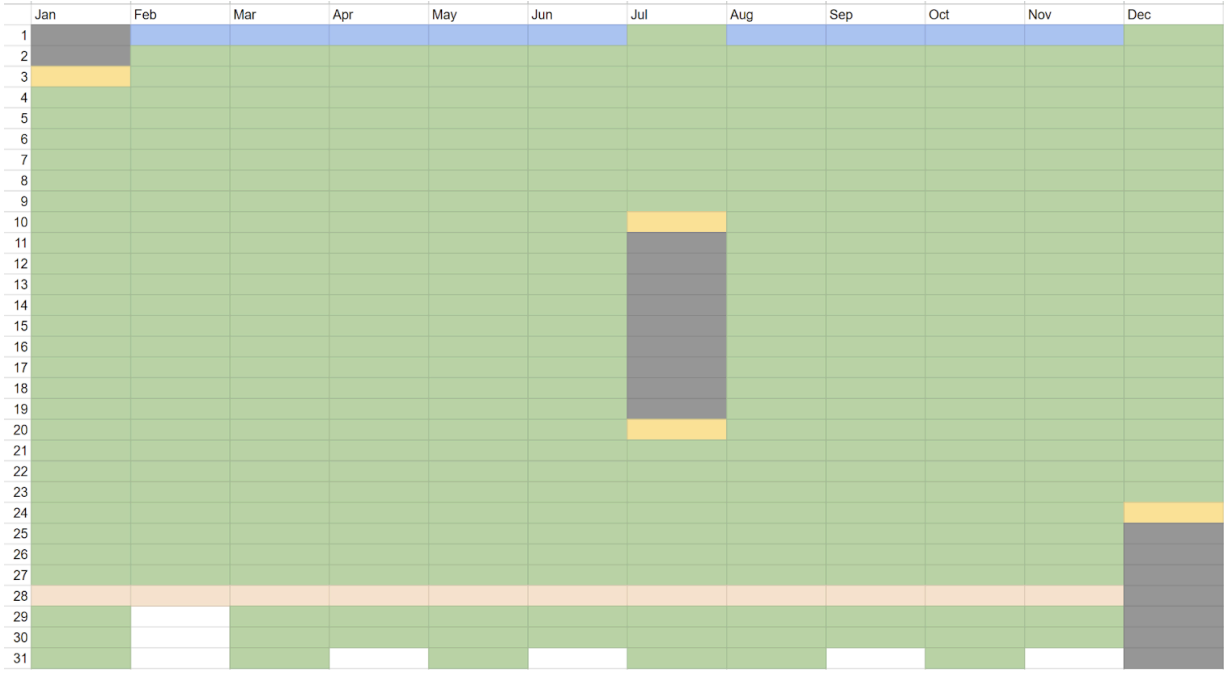

Figure 3-6-01: Plant Operation Schedule

4. Economic Considerations

This process was priced using a variety of sources. Older prices from research articles and websites which were expected to have experienced significant changes due to inflation were adjusted accordingly (AIER, 2024). Similarly, items and information priced with older textbooks and Capcost accounted for outdated costs through scaling with the Chemical Engineering Cost Plant Index (CEPCI) (The University of Manchester, n.d.), using 800 as 2024's CEPCI value. Aspen was also used where applicable.

4.1 Total Capital Cost

4.1.1 Land

As described above, based on existing water processing facilities in Sweden, our property will be on 27 acres of land. Land cost was determined using agricultural prices for production in Upper Norland (Statistikmyndigheten SCB, 2018), where our plant is located.

Table 4-1-1-01. Capital costs associated with land usage

Land Usage (acres)	Cost per Area ($/acres)	Total Cost
27	761.01	$20,547.23

4.1.2 Water Pretreatment Equipment Costs

The first step of water purification is the mesh screen with included pumps. This was priced as the RF100 Duplex Self-Cleaning Filter via Rotorflush (Rotorflush, n.d.), accounting for all 5 necessary pumps. The table below refers to this specific piece of equipment as a combination of both a pump and coarse filter, as represented in the water purification section's PFD. Because these filters included pumps and were a part of the water purification process, they

are not priced with all additional pumps within the *Ancillary Equipment Costs* (Section 4.1.6) portion of this paper.

Table 4-1-2-01. Cost for Inlet Pumps and Mesh Filters

Equipment	Base Cost	Quantity	Total Cost
P-100, F-100	$454.54	5	$2,272.70

The continuous rapid sand filter was priced under the assumption that the primary equipment cost was the shell of the filter. Because the equipment selected for this design is made from a plastic (FRP), a different, comparable plastic (high-density polyethylene) tank was used when selecting a vessel of the adequate volume for accurate shell pricing (Grainger, n.d.). The base price was then doubled to account for unincluded costs such as granular media (sand), and beyond.

Table 4-1-2-02. Cost for Continuous Rapid Sand Filter

Equipment	Base Cost	Scaling Factor	Total Cost
F-101	$2,685.87	2	$5,371.74

The stainless steel tank required to collect was priced via The Cary Company (The Cary Company, n.d.).

Table 4-1-2-03. Cost for Continuous Rapid Sand Filter Waste Tank

Equipment	Size	Quantity	Total Cost
T-100	37.95 L	1	$312.49

The UV disinfection tube cost was collected from US Water Systems (US Water Systems, n.d.) using their *60 GPM Polaris Scientific Ultraviolet Disinfection System - UVA-60B* model.

Table 4-1-2-04. Cost for UV Disinfection Tube

Equipment	Flow Capacity	Quantity	Total Cost
V-100	13,627 kg/hr	1	$3,977.80

The price of the GAC filter was determined via Crystal Quest Water Filters 60 GPM model (Crystal Quest Water Filters, n.d.) based on our system's required flowrate, and accounting for alternation required to maintain the GAC filters.

Table 4-1-2-05. Cost for Granular Activated Carbon (GAC) Filters

Equipment	Flow Capacity	Quantity	Total Cost
F-102	13,627 kg/hr	2	$9,638.00

Our reverse osmosis system was priced, again, with Crystal Quest Water Filters (Crystal Quest Water Filters, n.d.) using the 30,000 GPD model. Similarly, the price is dependent on both flow rate and the fact that 2 of 4 total RO systems will be run simultaneously, and rotated on a monthly basis.

Table 4-1-2-06. Cost for Reverse Osmosis (RO) Systems

Equipment	Flow Capacity	Quantity	Total Cost
F-103	6,548 kg/hr	4	$164,116.60

The final equipment in the water purification process is the water storage tank, used as a backup in case any prior step in the purification process undergoes unexpected shutdown. The tank was priced as a carbon steel tank with *Plant Design and Economics for Chemical Engineers* (Peters et al., 2003). As the figure used for this base cost was created in 2002, that year's CEPCI (395.6) was accounted for while scaling for total cost.

Table 4-1-2-07. Cost for Water Storage Tank

Equipment	Size	Base Cost	Scaling Factor	Total Cost
T-101	10,000 L	$11,250	800/395.6	$22,750.25

4.1.3 Electrolysis Equipment Costs

The cost of our PEM electrolysis unit was based off of flowrate requirements, while ensuring that we have a slight overcapacity for processing water into hydrogen and oxygen. The price to purchase electrolysis units (in bulk) which are capable of processing 1 kg/hr of water into high-purity hydrogen was determined using Alibaba (Alibaba, n.d.), and scaled accordingly to account for the total inlet flow rate to the electrolysis block.

Table 4-1-3-01. Cost for PEM Electrolysis Units

Equipment	Base Cost	Scaling Factor	Total Cost
R-100	$10,000	2,500	$25,000,000.00

4.1.4 Hydrogen Purification Costs

CapCost was used to price the compressor (carbon steel, centrifugal pump) used to compress and pump the hydrogen stream exiting electrolysis with a CEPCI of 800.

Table 4-1-4-01. Cost for Hydrogen Stream Compressor

Equipment	Power Requirement (kW)	Quantity	Total Cost
C-106	455	1	$304,000.00

Plant Design and Economics for Chemical Engineers (Peters et al., 2003) was used to price the condenser used to remove water from the hydrogen stream, priced as a multiple-pipe, carbon-steel heat exchanger.

Table 4-1-4-01. Cost for Hydrogen-Water Condenser

Equipment	Heat Exchange Area	Base Cost	Scaling Factor	Total Cost
H-108	24.8 m^2	$1,200.00	800/395.6	$2,426.69

The hydrogen pressure swing adsorption unit was priced using two major costs: the equipment itself (Alibaba, n.d.), constituent of 4 total columns, and the quantity of 5A zeolite required (40 kg) per each of the 4 columns (MSE Supplies LLC, n.d.). This produces the scaling factor of 160 shown below in the table. Due to the regeneration and longevity of its lifetime, zeolite is considered a one-time (capital) cost rather than a material or operating cost.

Table 4-1-4-02. Cost for Hydrogen Pressure Swing Adsorption

Equipment	Base Cost	Scaling Factor	Total Cost
5A Zeolite	$47.40/kg	160	$7,584.00
A-100	$9,500.00	N/A	$9,500.00

The final step of the hydrogen purification process is the multi-stage compressor. This was modeled in Aspen Plus v14 using three heat exchanger and three compressor blocks. Each of the compressor blocks were priced by Aspen's economic analysis tool, however the heat exchangers were priced separately as carbon steel, double pipe shell and tube heat exchangers using *Plant Design and Economics for Chemical Engineers* (Peters et al., 2003). Because figures in that textbook were produced in 2002, a CEPCI of 395.6 was used in scaling of the base cost. Additionally, the logarithmic scale of the figure used resulted in negligible price differences between the subtly different heat exchanger areas.

Table 4-1-4-03. Heat Exchanger Prices for Hydrogen Multi-Stage Compression

Equipment	Heat Exchange Area	Base Cost	Scaling Factor	Total Cost
H-102	3.55 m^2	$1,100.00	800/395.6	$2,224.47
H-103	3.52 m^2	$1,100.00	800/395.6	$2,224.47
H-104	3.63 m^2	$1,100.00	800/395.6	$2,224.47

Table 4-1-4-04. Compressor Prices for Hydrogen Multi-Stage Compression

Equipment	Total Cost
C-100	$1,907,400.00
C-101	$2,009,700.00
C-102	$2,000,000.00

4.1.5 Oxygen Purification Costs

CapCost was used to price the compressor (carbon steel, centrifugal pump) used to compress and pump the hydrogen stream exiting electrolysis with a CEPCI of 800. CapCost prices any compressor below a power requirement of 450 kW as the minimum compressor cost.

Table 4-1-5-01. Cost for Oxygen Stream Compressor

Equipment	Power Requirement (kW)	Quantity	Total Cost
C-107	160	1	$302,000.00

Plant Design and Economics for Chemical Engineers (Peters et al., 2003) was used to price the condenser used to remove water from the oxygen stream, priced as a double-pipe, carbon-steel heat exchanger.

Table 4-1-5-02. Cost for Oxygen Stream Condenser

Equipment	Heat Exchange Area	Base Cost	Scale Factor	Total Cost
H-109	3.56 m^2	$1,010.00	800/395.6	$2,042.47

The oxygen pressure swing adsorption unit was priced using two major costs: the equipment itself (Alibaba, n.d.), constituent of 2 total columns, and the quantity of 13X zeolite required (15 kg) per each of the columns (MSE Supplies LLC, n.d.). There are 4 total columns required for our process, producing the scaling factor of 60 shown for the zeolite below. Again, due to its ability to regenerate and longevity of its lifetime, purchase of the zeolite is considered a one-time (capital) cost rather than a material or operating cost.

Table 4-1-5-03. Cost for Oxygen Pressure Swing Adsorption

Equipment	Base Cost	Scaling Factor	Total Cost
13X Zeolite	$47.50/kg	60	$2,850.00
A-101	$4,000.00	2	$8,000.00

Unlike hydrogen's compression system, the multi-stage oxygen compression system (including all heat exchangers) was priced as one unit according to the 'mcompr' block in Aspen Plus v14. The table below represents this as the three compressors and heat exchangers shown in the oxygen purification system's PFD.

Table 4-1-5-04. Cost for Oxygen Multi-Stage Compression System

Equipment	Total Cost
C-103, H-105, C-104, H-106, C-105, H-107	$1,930,400.00

4.1.6 Ancillary Equipment Costs

All pumps, besides the inlet pumps which have attached filters, were priced using CapCost. These were priced as carbon steel, centrifugal pumps. Any pump with a shaft power under 1 kW was valued at the minimum purchase price, and any pump with a shaft power above 300 kW was valued using pumps in series. The value of the CEPCI for 2024 (800) was included in the calculation CapCost performed.

Table 4-1-6-01. Cost for Pumps Modeled in CapCost

Equipment	Shaft Power (kW)	Discharge Pressure (kPag)	Base Cost	Quantity	Total Cost
P-101	2.23	654.6	$8,341.00	2	$16,682.00
P-102	0.422	0	$7,650.00	2	$15,300.00
P-103	0.0087	0	$7,650.00	2	$15,300.00
P-105	0.129	0	$7,650.00	2	$15,300.00
P-106	0.211	0	$7,650.00	2	$15,300.00
P-107	6.03	810.6	$10,439.00	2	$20,878.00
P-108	0.253	101.325	$7,650.00	2	$15,300.00
P-110	0.00664	0	$7,650.00	2	$15,300.00
P-111	0.167	0	$7,650.00	2	$15,300.00
P-112	3.23	506.65	$8,933.00	2	$17,866.00
P-113	0.253	101.325	$7,650.00	2	$15,300.00
P-114	0.1	0	$7,650.00	2	$15,300.00

CapCost was additionally used to price the turbine used to burn purge hydrogen coming out of the PSA unit, assuming the turbine is 34.2% energy efficient. The turbine was valued as a stainless steel axial gas turbine.

Table 4-1-6-02. Cost for Turbine Modeled in CapCost

Equipment	Energy Produced (kW)	Total Cost
G-100	274	$509,625.00

The final pieces of ancillary equipment not already accounted for are the heat exchanger required to heat water pre-electrolysis, as well as the heat exchanger used to increase the temperature of hydrogen before PSA. The heat exchangers were priced as a carbon steel, double pipe shell and tube heat exchanger with *Plant Design and Economics for Chemical Engineers* (Peters et al., 2003), Table 14-15. CEPCI was accounted for in the scaling factor.

Table 4-1-6-03. Cost for Heat Exchangers

Equipment	Heat Exchange Area	Base Cost	Scaling Factor	Total Cost
H-100	1.00787 m^2	$1,000.00	800/395.6	$2,022.24
H-101	0.2169 m^2	$950.00	800/395.6	$1,921.13

4.1.7 Total Capital Costs

Total capital investment based on equipment cost was determined and scaled according to *Plant Design and Economics for Chemical Engineers* (Peters et al., 2003), following Table 6-9 as a fluid processing plant. Because there is no chemical inventory required for our process, working capital was assumed to include all costs associated with bottling. A breakdown of costs, along with total capital investment, is seen below.

Table 4-1-7-01. Breakdown of Total Capital Investment

Direct Costs	
Purchased Eqpt. Delivered	$34,695,057.76
Purchased Eqpt. Installation	$16,306,677.15
Instrumentation and Controls	$12,490,220.79
Piping	$23,592,639.28
Electric Systems	$3,816,456.35
Buildings (including services)	$6,245,110.40
Yard Improvements	$3,469,505.78
Service Facilities	$24,286,540.43
Total Direct Plant Cost	**$124,902,207.93**
Indirect Costs	
Engineering and Supervision	$11,449,369.06
Construction Expenses	$14,224,973.68
Legal Expenses	$1,387,802.31
Contractor’s Fee	$7,632,912.71
Contingency	$15,265,825.41
Total Indirect Plant Cost	**$49,960,883.17**
Fixed Capital Investment (FCI)	$174,863,091.10
Working Capital (15% total investment)	$30,878,601.40
Total Capital Investment	**$205,741,692.50**

4.2 Yearly Operating Costs

4.2.1 Raw Material Costs

The only inlet material stream required for this process is water to be pumped from the Torne river. Total yearly flow was determined by averaging the backwashing and non-backwashing flow rates in conjunction with pricing information for process water from Peters et al. (2006), assuming the price of process water is equal to the price paid to the municipality of Sweden where the river water is taken from. The price used in calculations has already been scaled to account for the CEPCI in 2006 (500) of 0.05 cents per kg.

Table 4-2-1-01. Cost for Inlet Water

Base Cost	Total Material	Total Yearly Cost
$0.0008/kg	72,116,315 kg	$57,693.05

Beyond water, membranes used within equipment should be replaced within a certain timeline. As stated in sections above, electrolysis *Nafion* membranes (Ion Power, n.d.) require replacement every 5 years, GAC membranes (Crystal Quest Water Filters, n.d.) every year, and RO membranes (Espwater, n.d.) every 4 years. The PEM electrolysis unit has 125 stacks, with 50 cells per stack, each containing one membrane. The two GAC filters each have 1 membrane, whereas each of the four RO units have 16 membranes.

Table 4-2-1-02. Cost for Membrane Replacements

Membrane Type	Base Cost	Filters Required	Scale Factor	Total Yearly Cost
Nafion	$270.00	6,250	1/5	$339,290.60
GAC	$19.75	2	1	$39.50
RO	$369.00	56	1/4	$5,166.00

4.2.2 Utility Costs: Onshore Wind Electricity

All electricity from this system is sourced from onshore wind in Sweden. Converting from Euros to USD, the cost for onshore wind electricity was found to be 0.038 USD/kWh (Swedish Wind Energy Association, n.d.). Any major equipment with electricity requirements is shown below. Scaling factor is based on the number of equipment items in the system; i.e, two RO units are always run simultaneously, and therefore electricity requirements are given on a per-unit basis. The energy requirements for the PSA units is an hourly average based on the changing start up and shut-down electricity needs.

Table 4-2-2-01. Onshore Wind Electricity Costs for Major Equipment

Equipment	Electricity Requirement (kW)	Scale Factor	Operational Hours	Total Yearly Cost
P-100, F-100	0.380	4	8,000	$462.08
F-101	225	1	8,000	$68,400.00
V-100	0.039	1	8,000	$11.86
F-103	2.25	2	8,000	$1,368.00
R-100	100	125	8,000	$3,800,000.00
C-106	455	1	8,000	$138,320.00
A-100	17.2	1	8,000	$5,228.80
C-100, H-102, C-101, H-103, C-102, H-104	438	1	8,000	$133,152.00
C-107	160	1	8,000	$48,640.00
A-101	7.28	1	8,000	$2,213.12
C-103, H-105, C-104, H-106, C-105, H-107	227	1	8,000	$69,008.00

Similarly, energy requirements for pumps (other than inlet because of its attached screen) are shown in the table below.

Table 4-2-2-02. Onshore Wind Electricity Costs for Pumps

Equipment	Electricity Requirement (kW)	Operational Hours	Total Yearly Cost
P-101	2.23	8,000	$677.92
P-102	0.422	8,000	$128.42
P-103	0.00867	8,000	$2.64
P-105	0.129	8,000	$39.22
P-106	0.211	8,000	$64.14
P-107	6.03	8,000	$1,833.12
P-108	0.253	8,000	$76.91
P-110	0.00664	8,000	$2.02
P-111	0.167	8,000	$50.77
P-112	3.23	8,000	$981.92
P-113	0.253	8,000	$76.91
P-114	0.1	8,000	$30.40

4.2.3 Utility Costs: Cooling River Water

Cooling river water required to be pumped into the system (as a utility) was priced using values for process water from Peters et al. (2006).

Table 4-2-3-01. Cooling River Water Costs for Overall Process

Equipment	Base Cost	Water Requirement (kg/hr)	Operational Hours	Total Yearly Cost
H-102, H-103, H-104	$0.0008/kg	6,000 (2,000 each)	8,000	$38,400.00
H-105, H-106, H-107	$0.0008/kg	6,000 (2,000 each)	8,000	$38,400.00
H-108	$0.0008/kg	5,000	8,000	$32,000.00
H-109	$0.0008/kg	4,000	8,000	$25,600.00

4.2.4 Labor Costs

Total labor costs were determined using Figure 6-8 in *Plant Design and Economics for Chemical Engineers* (Peters et al., 1991), using an anticipated production rate of around 50 tons daily, and assuming operators are required 365 days per year for 13 processing steps to get the total number of operators. Operator pay rate was determined to be around $38.12 per hour (US Bureau of Labor Statistics, 2023). Supervisor pay was assumed to be 20% of total operator cost yearly.

Table 4-2-4-01. Overall Labor Costs

Labor Source	Number	Total Yearly Cost
Operators	65	$5,064,623.20
Supervisors	11	$1,012,924.64

4.2.5 Operating Costs and Product Revenue

In the table below, total operating costs are summarized to include raw materials, electricity, and utility water consumption.

Table 4-2-5-01. Overall Operating Costs

Operating Cost	Total Yearly Cost
Raw Materials	$402,189.15
Utility: Onshore Wind Electricity	$4,270,768.25
Utility: Cooling River Water	$134,400.00
Total	**$4,807,357.40**

Additionally, revenues from hydrogen and oxygen are listed below. Hydrogen prices were collected from Azo Materials (Azo Materials, 2020), whereas oxygen was priced using data from Sci Analytical Laboratories (SCI Analytical, n.d.).

Table 4-2-5-02. Overall Revenue

Product	Wholesale Price	Quantity Produced	Total Yearly Revenue
Microelectronics-Grade Hydrogen	$212.59/kg	1,864,000 kg	$394,413,880.66
Research-Grade Oxygen	$2.94/kg	15,334,000 kg	$45,109,684.35
Total			**$439,523,565.01**

4.2.6 Taxes and Other Fees

The remaining operating costs include waste disposal taxes, insurance costs, property taxes, and maintenance fees. The total yearly SPM removal (coming from the continuous sand filter) is a function of taxes currently set in place in Sweden for biodegradable landfill (European Environment Agency, 2023). Insurance was valued at 1% of total FCI, and similarly maintenance fees at 4% FCI (Peters et al., 1991). Property taxes in Sweden, assuming our plant is considered an industrial property, cost 5% of FCI (Skatteverket, n.d.). Income taxes and depreciation will be discussed in section 4.3 below.

Table 4-2-6-01. Taxes and Other Fees

Expense	Total Yearly Cost
Disposal Taxes	$19.76
Insurance Costs	$1,748,630.91
Property Taxes	$874,315.46
Maintenance Fees	$6,994,523.64

4.3 Cash Flow Analysis

A cash flow analysis was conducted to determine if our green hydrogen production plant should ultimately be built and operated or not. This factors in a 20.6% yearly corporate income tax (PWC, n.d.), and a 10-year straight line depreciation from years 1-10. Our plant was assumed to have a 20-year lifetime, with an 18-month start-up period. In year -1, two-thirds of the total capital investment is spent. For the first six months of year 0, the remaining third of capital investment is spent, while for the remaining half of the year the plant is operational at half total capacity. At year 20, the plant is shut down, and some capital costs are recuperated by selling all pumps, RO units, multistage compressors, the turbine, and land. The actual cash flow table is shown below for the plant's lifetime.

Table 4-3-01. Actual Cash Flow

Year	Actual Cash Flow
-1	-$134,922,082.27
0	$32,175,574.07
1-10	$336,883,157.20
11-19	$332,698,705.60
20	$341,707,093.84
Sum After 20 Years Operation	**$6,602,618,780.62**

Discounted cash flow (DCF), as a method of assessing previous and future value of an investment is another key component in the go-no-go decision for a chemical operating plant. Setting a discount hurdle rate of 18%, due to the relative novelty of this process, but lack of safety or market risks, gives us the graph displaying DCF below. This DCF scenario has a net present value (NPV) of around $1.38 billion.

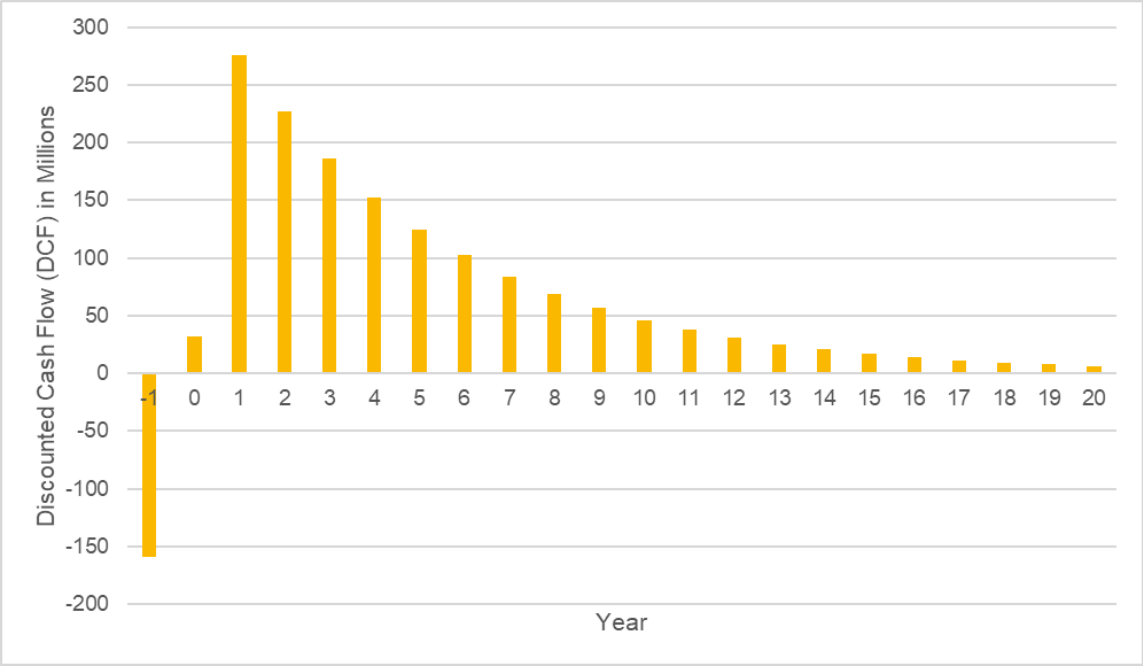

Figure 4-3-01: Discounted Cash Flow (DCF) at Hurdle Rate

Setting the NPV to zero, the internal rate of return can be calculated (via Excel) to be 64%. To further confirm our profitability, return on investment (ROI) was calculated as the ratio of the net return to the cost of investment, giving a ROI of 32.1. Because, jointly, the ACF shows extreme profitability after 20 years, the hurdle discount rate is lower than the calculated IRR, and the ROI is greater than one, this process is economically viable and should be executed.

4.3.1 Alternate Scenario: Lower-Grade Hydrogen Production

Although an IRR of 64% is possible, it is slightly larger than what is anticipated of a green hydrogen plant. This number likely holds the greatest dependence on the price of microelectronics-grade hydrogen, which could be susceptible to changes if the existing market fluctuates in value. Therefore, another cash flow analysis is shown in the table below using the

scenario that our hydrogen produced only meets 99.99% purity, and is sold at half the price ($106.30/kg) (Azo Materials, n.d.).

Table 4-3-1-01. Actual Cash Flow for Lower-Grade Hydrogen Production

Year	Actual Cash Flow
-1	-$134,922,082.27
0	-$17,126,161.01
1-10	$180,354,673.84
11-19	$176,116,394.97
20	$185,124,783.21
Sum After 20 Years Operation	**$3,421,670,833.03**

The discounted cash flow within our plant's lifetime for this scenario is shown below, assuming the same hurdle rate of 18%.

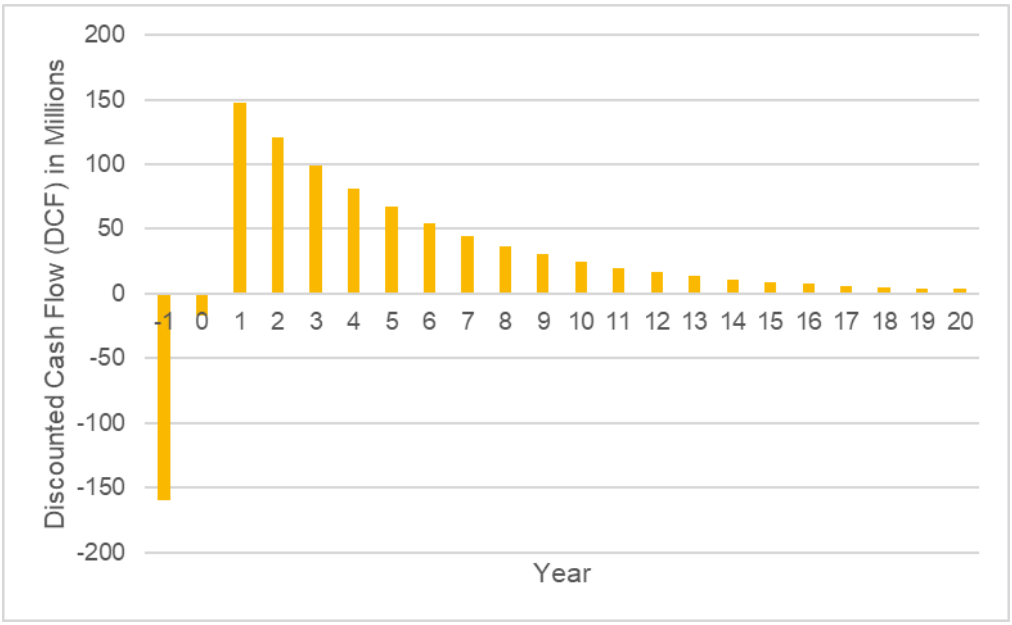

Graph 4-3-1-01: Discounted Cash Flow (DCF) at Hurdle Rate for Alternate Scenario

Using the same calculations as above by setting the NPV to zero, we calculate that the IRR of this alternate scenario is roughly 46%. As a result, we can conclude that despite hydrogen being sold at half of the price per kilogram, our process still proves to be financially viable with an IRR above the hurdle discount rate, and a positive ACF after 20 years of operation.

4.3.2 Alternate Scenario: Transportation Fees

One key economic assumption in our profitability is the ability to co-locate with a microelectronics production facility. This removes high fees associated with the transportation of hydrogen, which is extremely dangerous and therefore challenging to ship. In the scenario where this co-location was not possible, a cash flow analysis was conducted in the same manner as demonstrated above, using a hurdle rate of 18%. Including a capital cost of $26 million dollars for port and harbor construction, operating costs of $27 million dollars yearly for port and harbor

maintenance, and $50 million dollars yearly for shipping hydrogen (using a rate of $26.68 per kg, shipping 3000 km), it was determined that our process was still economically feasible. The port and harbor construction costs were estimated using the upper estimate of the range provided by Fin Models Lab (Ryzhkov, 2024). The transportation cost rate was overestimated with the goal of performing a conservative economic sensitivity analysis. The highest transportation rate of 2.668 per kg, per 3000 km, was multiplied by 10 to get our transportation rate (Blanco, 2022). At the end of the plant lifetime, profit is expected to reach $2.2 billion dollars, with a calculated ROI of 9.5, and IRR of 37%.

5. Safety and Environmental Concerns

5.1 Safety Concerns

This process does not have many safety concerns due to the main components of the system being water, oxygen gas, and hydrogen gas. The water does not provide any safety concerns. The oxygen gas supports combustion as it is one of the three legs of the fire triangle. An oxygen gas leak should be properly ventilated while ensuring that all fuel and ignition sources are avoided in order to minimize the risk associated with this leak.

The hydrogen gas provides the greatest safety concerns for this process due to its flammability and explosivity risks. The most credible safety event surrounding this concern is a gasket failure in the hydrogen compressor which results in a jet fire that was modeled in ALOHA, shown in Figure 5-1-01.

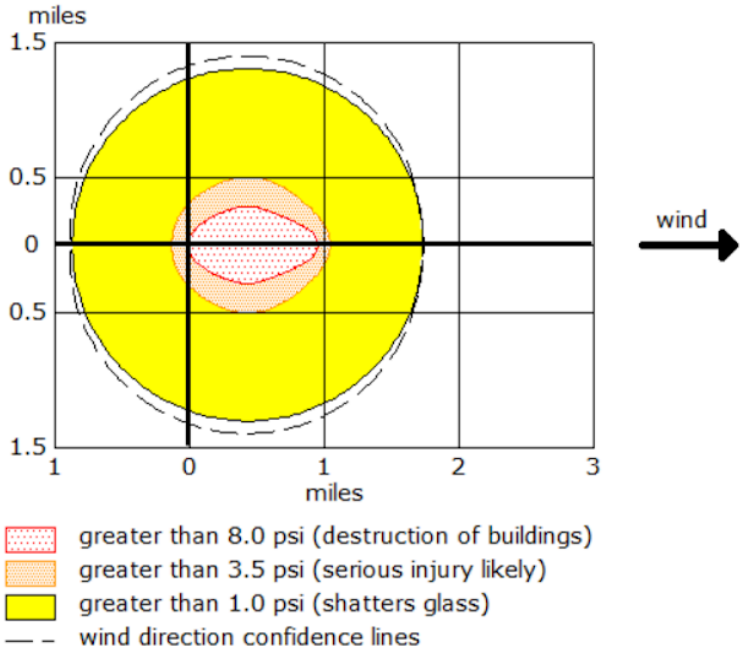

Figure 5-1-01: ALOHA Modelling for Hydrogen Explosion

The most conservative estimations were used in order to model the worst case scenario regarding this safety concern. The compressed hydrogen gas that is leaving the final compressor in the hydrogen purification process was determined to pose the greatest risk. This was modeled to flow through a 5.3 inch diameter pipe that is 100 feet long. The atmospheric conditions in Abisko, Sweden were found to fall under stability class C as there were 8.6 mph winds, 93% humidity, temperatures as low as -7.9°C, and partial cloud coverage.

Since our plant is located in a congested area due to the surrounding trees and equipment, the potential blast associated with this event would cause the destruction of buildings within a mile by half mile area, serious injuries within a mile by mile area, and the shattering of glass within a two mile by three mile area.

5.2 Environmental concerns

This process contains a few environmental concerns that had to be considered. First, the water purification process produces a concentrated sludge waste after the continuous rapid sand filter. While the European Union is looking into adopting protocols that require advanced sludge treatment technologies that remove toxic compounds and have better odor control in the distant future, this is not a concern of our plant as it only produces about 440 kg of waste per year. This was determined by finding the exit waste stream per hour by completing a material balance around the operating unit then multiplying it out by 8000 hrs. At this amount, it is able to be disposed of in a landfill.

The standards set by the European Union for wastewater treatment and disposal vary on a case by case basis. They require that companies must obtain permits or authorizations from authorities before discharging wastewater into rivers. These permits specify discharge limits

along with other conditions that need to be met to ensure compliance with the regulations set in place. While that is the case, we can assume that we will not be violating any environmental safety requirements by disposing of this wastewater into the Torne river as it should have less organic contaminants and suspended solids than the amounts specified by the European Union in the Urban Waste Water Treatment Directive. In 2039, they will implement greater restrictions on the nitrogen and phosphorus contents of the waste water, so our process may have to be re-evaluated at that time. Additionally, the cooling water streams leave the system at 86.6°C; before they can be returned to the river, they must be mixed with cooler water to protect the wildlife in the river.

Since the hydrogen purge stream is burned off and sent to an axial gas turbine, there are no environmental concerns with this process due to it being a clean conversion of the hydrogen waste product. The hydrogen purge waste stream is burned by a furnace to generate electrical energy, so none of it will be released or flared to the atmosphere. The oxygen purge waste that is vented to the atmosphere is not of any environmental concern as it only contains trace amounts of contaminants that are already found in the atmosphere.

5.3 Societal Concerns

As mentioned in the safety section, there would be concerns regarding hydrogen safety as there is potential for an explosive event occurring. This would cause concern for those living within a few miles of the plant as their homes and lives would potentially be at risk. This could cause insurance prices to increase while also causing property values to decrease. While that is the case, this plant as it is currently designed would create many jobs in Abisko, Sweden. The total cost of operators would be over five million dollars, as operators would make around $38

per hour, and the total cost of supervisors would be over one million dollars. Average wages in Sweden were reported to be about $2,800 per month (Horizons, 2023), so this project would provide a significant pay raise for many of the workers in the area, boosting the surrounding area's economy.

Furthermore, the surrounding community could be upset due to the nearly thirty acres of land being taken up near the Torne River for a chemical plant rather than it being used for residential or commercial construction among other applications.

6. Conclusions and Recommendations

After analysis of the entire process and conducting an economic evaluation, we recommend that this process moves forward. This project offers numerous benefits and opportunities, both to the local economy in Sweden and the world as a whole. Firstly, the process is extremely profitable, generating 6.6 billion dollars in revenue by the end of the 20-year plant lifetime. The profitability of this project also lends itself to boosting the local economy through the generation of jobs and the above-average salary provided to the workers. Secondly, this process is entirely carbon-neutral, helping to reduce greenhouse gas emissions and assist in the fight against climate change. We are, therefore, hopeful that this process can ultimately serve as the pioneer project which transitions industrial hydrogen production away from fossil-fuel based processes, and towards green processes like our own.

Despite the promising outlook of this project, there is still room for improvement both in terms of design and increasing profitability. One key assumption we made was that the electrodes would last the lifespan of the facility. One consideration for future designs would be to obtain good data on electrode lifespans and maintenance timelines. This would likely add to operating costs and decrease the final internal rate of return, but we could not make accurate estimations of the electrode lifespan at present. Furthermore, RO modeling proved to be difficult, and therefore values for rejection rates were taken from literature. For a more accurate estimate in future work, RO modeling should be conducted using manufacturer-provided softwares. Additionally, an analysis should be conducted to determine if selling oxygen at research-grade purity (99.999%) with the operation of a condenser generates a greater profit than selling the oxygen at a lower, medical-grade purity (99.5%) without the condenser. With these design

suggestions in mind, we are confident in the current and future potential of our green hydrogen production plant to succeed.

7. Acknowledgements

We would like to acknowledge Professor Anderson for the time he has offered us as our course instructor. We would further like to thank Professor Geise and Unnerstall for the insights they have provided in water purification and safety, respectively.

References

Abisko, Sweden. (n.d.). Google Earth. https://earth.google.com/web/search/Abisko,+Sweden/@68.34941085,18.8300442,380.18169015a,755.1159761d,35y,66.31721418h,44.99040095t,0r/data=CnkaTxJJCiUweDQ1ZGE0NWI1YzIzOWU4NDE6MHg0YzE1YWY1ODk3YmQyMzQ2GbGmDeJeFlFAIdMZczLM1DJAKg5BYmlza28sIFN3ZWRlbhgCIAEiJgokCeJjUPgbX09AEesGqPqUr0pAGXojnj0nL0RAIfDG9Fp_8A_AOgMKATA

AIER. (2024, March 21). Cost of living calculator: What is your dollar worth today? https://www.aier.org/cost-of-living-calculator/?utm_source=Google%20Ads&utm_medium=Google%20CPC&utm_campaign=COLA&gad_source=1&gclid=Cj0KCQjw8J6wBhDXARIsAPo7QA9ALgBinUopHH9Zc-MEoDK6hh9xqxdNCqK4D47GBPl1YX29eRYP2BgaAreVEALw_wcB

Alibaba. (n.d.). H2 gas producing 1 -200nm3 /H Pem high purity 99.999% Pem fuel cell hydrogen generator water Electrolyzer. Alibaba.com: Manufacturers, Suppliers, Exporters & Importers from the world's largest online B2B marketplace. https://www.alibaba.com/product-detail/H2-gas-producing-1-200Nm3-h_1600897837453.html?spm=a2700.7724857.0.0.21c3379cKlY3mu

Alibaba. (n.d.). High purity Psa hydrogen purifier. Alibaba.com: Manufacturers, Suppliers, Exporters & Importers from the world's largest online B2B marketplace. https://www.alibaba.com/product-detail/Pressure-Swing-Adsorption-For-Hydrogen-Production_1601033673944.html?spm=a2700.galleryofferlist.p_offer.d_image.5ed651bf4H5ITa&s=p

Alibaba. (n.d.). Nuzhuo 3nm3/H-150nm3/H pressure swing adsorption oxygen gas producing machine for medical use - Buy oxygen gas producing Machine,Swing adsorption oxygen gas producing Machine,Oxygen gas producing machine for medical use product on Alibaba.com. Alibaba.com: Manufacturers, Suppliers, Exporters & Importers from the world's largest online B2B marketplace. https://www.alibaba.com/product-detail/NUZHUO-3Nm3-H-150Nm3-H-Pressure_1600958758564.html?spm=a2700.galleryofferlist.p_offer.d_image.844f5ff7QfzoFy&s=p

Average salary in Sweden & stockholm - median income 2024. *Horizons*. (2024). https://joinhorizons.com/countries/sweden/hiring-employees/average-salary/

Azhagapillai, P., Khaleel, M., Zoghieb, F., Luckachan, G., Jacob, L., & Reinalda, D. (2022). Water vapor adsorption capacity loss of molecular sieves 4A, 5A, and 13x resulting from methanol and heptane exposure. *ACS Omega*, 7(8), 6463–6471. https://doi.org/10.1021/acsomega.1c03370

Badgett, A., Pivovar, B., & Ruth, M. (n.d.). *Operating Strategies for Dispatchable PEM Electrolyzers That Enable Low-Cost Hydrogen Production.*

Blanco, H. (2022, May 4). What's best for hydrogen transport: Ammonia, liquid hydrogen, LOHC or pipelines? Energy Post. https://energypost.eu/whats-best-for-hydrogen-transport-ammonia-liquid-hydrogen-lohc-or-pipelines/

BloombergNEF. (2023, August 9). Green hydrogen to undercut gray sibling by end of decade. https://about.bnef.com/blog/green-hydrogen-to-undercut-gray-sibling-by-end-of-decade/

Case study report for the Xylem HT-BTES plant in Emmaboda, Sweden. *Heat Pumping Technologies*. (n.d.). https://heatpumpingtechnologies.org/annex52/wp-content/uploads/sites/60/2022/01/anderssonetal2021case-study-report-annex-52ht-btes-xylemswedenfinal.pdf

Cigal, J.-C. (n.d.). Expanding use of hydrogen in the electronics industry. https://www.linde-gas.com/en/images/Expanding%20Use%20of%20Hydrogen%20in%20the%20Electronics%20Industry%20Gasworld%20November%202016_tcm17-418683.pdf

Climate Data. (n.d.) Tornio climate: Average Temperature by month, *Tornio water temperature*. https://en.climate-data.org/europe/finland/tornio/tornio-9803/#google_vignette

Climate Data. (n.d.). Abisko climate: Average Temperature by month, *Abisko water temperature*. https://en.climate-data.org/europe/sweden/norrbottens-laen/abisko-291585/

CO2 Meter. (n.d.). *Oxygen Purity Grade Chart.* https://www.co2meter.com/blogs/news/oxygen-purity-grade-charts

Crystal Quest Water Filters. (n.d.). Commercial reverse osmosis system. https://crystalquest.com/products/reverse-osmosis-system-high-flow?variant=8111923724402

Crystal Quest Water Filters. (n.d.). Eagle redox alloy® 6500 (per pound). https://crystalquest.com/products/eagle-redox-alloy-6500

Crystal Quest Water Filters. (n.d.). Granular activated carbon water filtration system.

https://crystalquest.com/products/gac-water-filtration-system?variant=2135594532874

Emam, A. S., Hamdan, M. O., Abu-Nabah, B. A., & Elnajjar, E. (2024). A review on recent trends, challenges, and innovations in alkaline water electrolysis. *International Journal of Hydrogen Energy*, *64*, 599–625. https://doi.org/10.1016/j.ijhydene.2024.03.238

Espwater. (n.d.). Axeon HF1-4040 RO membrane 150 PSI 2500 GPD 4" X 40" 200379. *ESPWaterProducts.com*. https://www.espwaterproducts.com/axeon-hf1-4040-4-x-40-2500-gpd-ro-membrane-150psi-200379/

European Environment Agency. (2023) Early warning assessment related to the 2025 targets for municipal waste and packaging waste. https://www.eea.europa.eu/publications/many-eu-member-states/early-warning-assessment-related-to

Falcão, D. S., & Pinto, A. M. F. R. (2020). A review on PEM electrolyzer modelling: Guidelines for beginners. *Journal of Cleaner Production*, 261, 121184. https://doi.org/10.1016/j.jclepro.2020.121184

Fresh Water Systems. (n.d.). Activated carbon filters 101. https://www.freshwatersystems.com/blogs/blog/activated-carbon-filters-101#:~:text=Change%20your%20carbon%20filter%20every%20six%20months%20to%20one%20year

Gasco 158: Oxygen (O2) 99.999% Vol. Calibration gas. (n.d.). *SCI Analytical*. https://scicalgas.com/product/gasco-158-oxygen-o2-99-999-vol-calibration-gas/

Grainger. (n.d.). SNYDER INDUSTRIES Storage Tank: Single Wall, Vertical, 500 gal, Closed Top, 3/16 in Wall Thick, HDPE. *Grainger Industrial Supply - MRO Products, Equipment and Tools*. https://www.grainger.com/product/2ZRD3?gucid=N:N:PS:Paid:GGL:CSM-2295:4P7A1P:20501231&gad_source=4&gclid=CjwKCAjw17qvBhBrEiwA1rU9w7aHN96jDVklLhfzm4hhCmvMGBeDchcc82BPjEKnqPEO2ywQa3N33RoC4CQQAvD_BwE&gclsrc=aw.ds

Hydrogen supply for semiconductor production. (2020, April 2). *Azo Materials*. https://www.azom.com/article.aspx?ArticleID=13297 and density

Hydrogen. (2022, January 14). *Keen Compressed Gas Co*. https://keengas.com/gases/hydrogen/

IEEE. Green hydrogen: The Swiss Army Knife of Energy Transition. *IEEE Smart Grid*. (n.d.). https://smartgrid.ieee.org/bulletins/march-2023-1/green-hydrogen-the-swiss-army-knife-of-energy-transition#:~:text=The%20market%20size%20for%20green%20hydrogen%20in%20the%20microchip%20industry,reach%20%243.6%20billion%20by%202030.

Ion Power. (n.d.). Nafion™ Membranes. https://ion-power.com/product/nafion-membranes/

Javadi, E. (n.d.). Adsorption isotherm of O 2 , N 2 and AR on zeolite 5A and 13x at ... https://www.researchgate.net/figure/Adsorption-isotherm-of-O-2-N-2-and-Ar-on-zeolite-5A-and-13X-at-29315K_fig3_257546882

Kumar, P., Bharti, R., Kumar, V., & Kundu, P. (2018). Polymer Electrolyte Membranes for

Microbial Fuel Cells: Part A. Nafion-Based Membranes—*ScienceDirect*. https://www.sciencedirect.com/science/article/abs/pii/B978044464017800004X

Länsstyrelsen. (n.d.). The River Torne International Watershed. https://catalog.lansstyrelsen.se/store/31/resource/201

Luberti, M., & Ahn, H. (2022). Review of polybed pressure swing adsorption for hydrogen purification. *International Journal of Hydrogen Energy*, 47(20), 10911–10933. https://doi.org/10.1016/j.ijhydene.2022.01.147

MESA Gas. (n.d.). Pure oxygen cylinders, instrument grade pure gases, research grade gases oxygen. https://mesagas.com/oxygen/

Miller, A. (2024, March 29). Best sand for pool filter: A guide for your next replacement. Hyclor. https://hyclor.com.au/best-sand-for-pool-filter/#:~:text=20%20Silica%20Sand%20is%20the,and%200.55mm%20in%20diameter

MSE Supplies LLC. (n.d.). 5A Zeolite. https://www.msesupplies.com/products/1kg-molecular-sieve-5a-pellets-spherescurrency=USD&variant=31758471331898&utm_medium=cpc&utm_source=google&utm_campaign=Google%20Shopping&stkn=00e3db816675&campaignid=21030333111&adgroupid=&keyword=&device=c&gad_source=1&gclid=Cj0KCQjwncWvBhD_ARIsAEb2HW9nUyj5uYfHBSis-zUTDqH6-tpGBop9x5B35CmVQ2jXmN6OZEHAtEcaAk8yEALw_wcB

MSE Supplies LLC. (n.d.). MSE PRO 1 kg molecular sieves 13X beads.

https://www.msesupplies.com/products/1kg-molecular-sieves-13x-pellets-spheres?currency=USD&variant=31758805205050&utm_medium=cpc&utm_source=google&utm_campaign=Google%20Shopping&stkn=00e3db816675&campaignid=15502649027&adgroupid=&keyword=&device=c&gad_source=1&gclid=Cj0KCQjwncWvBhD_ARIsAEb2HW8OY8oMri-w0JYk4VoQFIc5Xkbhtq7hI7SM3SxG4asaHjv1SopB824aAmjlEALw_wcB

Municipal and national property tax. *Skatteverket*. (n.d.). https://skatteverket.se/servicelankar/otherlanguages/inenglishengelska/individualsandemployees/declaringtaxesforindividuals/owningrealpropertyinswedenlivingabroad/municipalandnationalpropertytax.4.676f4884175c97df41923c6.html

Nikolic, D., Giovanoglou, A., Georgiadis, M. C., & Kikkinides, E. S. (2000). Hydrogen purification by Pressure Swing Adsorption. *Separation Science and Technology*, 35(5), 667–687.

NIWA. (n.d.). The Norwegian river monitoring programme – water quality status and trends in 2018. https://www.vannportalen.no/globalassets/publikasjoner/m1508/m1508.pdf

Norrgård, S., & Helama, S. (2022). Tricentennial trends in spring ice break-ups on three rivers in northern Europe. *The Cryosphere*, 16(7), 2881–2898. https://doi.org/10.5194/tc-16-2881-2022

Office of Energy Efficiency and Renewable Energy. (n.d.). Technical targets for membrane electrolysis. *Energy.gov*. https://www.energy.gov/eere/fuelcells/technical-targets-proton-exchange-membrane-electrolysis

Parkson. (n.d.). DynaSand® - Continuous backwash filter. *Parkson Corporation*. https://www.parkson.com/products/dynasand

PEM Electrolysis System—MATLAB & Simulink. (n.d.). Retrieved February 16, 2024, from https://www.mathworks.com/help/simscape/ug/pem-electrolysis-system.html

Peters, M. S., & Timmerhaus, K. D. (1991). *Plant Design and Economics for Chemical Engineers, Fourth Edition.* McGraw-Hill.

Peters, M. S., Timmerhaus, K. D., & West, R. E. (2003). *Plant Design and Economics for Chemical Engineers, Fifth Edition.* McGraw-Hill.

Peters, M. S., Timmerhaus, K. D., & West, R. E. (2006). *Plant Design and Economics for Chemical Engineers.* McGraw-Hill.

Power Engineering. (n.d.). New Benchmarks for Steam Turbine Efficiency. https://www.power-eng.com/news/new-benchmarks-for-steam-turbine-efficiency/#gref

Process Sensing Technologies. (n.d.). Impurities in Electronic Specialty Gases. https://www.processsensing.com/en-us/blog/sub-ppb-impurity-detection-electronic-specialty-gases.htm

PWC. Sweden. Corporate - Taxes on corporate income. (n.d.). https://taxsummaries.pwc.com/sweden/corporate/taxes-on-corporate-income

Renewable hydrogen for sustainable ammonia production. *AIChE*. (2019, August 2). https://www.aiche.org/resources/publications/cep/2019/august/renewable-hydrogen-sustainable-ammonia-production

Roadmap 2040. Swedish Wind Energy Association. (n.d.). https://swedishwindenergy.com/wp-content/uploads/2021/01/Roadmap-2040-ENG-rev-2020.pdf

Rotorflush. (n.d.). Rf100. Self-Cleaning Filters, Eel Screens, Submersible Pumps & Self-cleaning Filters | *Rotorflush*. https://www.rotorflush.com/products/rf100

Ryzhkov, A. (2024, April 4). *How much does it cost to start a port and Harbor Business: Unveiling capex and startup costs*. FinModelsLab. https://finmodelslab.com/blogs/startup-costs/port-harbor-startup-costs

Shiva Kumar, S., & Lim, H. (2022). An overview of water electrolysis technologies for green hydrogen production. *Energy Reports*, 8, 13793–13813. https://doi.org/10.1016/j.egyr.2022.10.127

Slanger, D. (2022). Run on less with hydrogen fuel cells. *RMI*. https://rmi.org/run-on-less-with-hydrogen-fuel-cells/#:~:text=In%20electrical%20terms%2C%20the%20energy,12%E2%80%9314%20kWh%20per%20kg.

Smith, R. A. (n.d.). Hydrogen purity standard. *Energy.gov*. https://www1.eere.energy.gov/hydrogenandfuelcells/pdfs/fp_workshop_smith.pdf

Son, K. N., Richardson, T.-M. J., & Cmarik, G. E. (2019). Equilibrium adsorption isotherms for H2O on zeolite 13X. *Journal of Chemical & Engineering Data*, *64*(3), 1063–1071. https://doi.org/10.1021/acs.jced.8b00961

Statistikmyndigheten SCB. (n.d.). Agricultural Land Prices 2018.

https://www.scb.se/contentassets/c2d67b4fcbdd456190889dd3523128c3/jo1002_2018a01_sm_jo38sm1901.pdf

Sweden. European Environment Agency. (2023, June 8). https://www.eea.europa.eu/publications/many-eu-member-states/sweden/view

Talu, O., Li, J., Kumar, R., Mathias, P. M., Moyer, J. D., & Schork, J. M. (1996). Measurement and analysis of oxygen/nitrogen/ 5A-zeolite adsorption equilibria for air separation. Gas Separation & Purification, 10(3), 149–159. https://doi.org/10.1016/0950-4214(96)00014-x

The Atmosphere | National Oceanic and Atmospheric Administration. (2023, July 28). *NOAA*. Retrieved April 2, 2024, from https://www.noaa.gov/jetstream/atmosphere

The Cary Company. (n.d.). 10 gallon stainless steel drum, UN rated, cover W/Bolt ring. https://www.thecarycompany.com/10-gallon-stainless-steel-drum?utm_source=google_shopping&gad_source=1&gclid=Cj0KCQjwk6SwBhDPARIsAJ59Gwd1IQE-fvOkAIlOrwverDlwnXXKAXhBenquf-CYkEBgHYtTtNiiANMaAo9FEALw_wcB

The University of Manchester. (n.d.). *Chemical Engineering Plant Cost Index*. https://personalpages.manchester.ac.uk/staff/tom.rodgers/Interactive_graphs/CEPCI.html?reactors/CEPCI/index.html

Towler, W., & Sinnott, R. K. (2008). *Chemical Engineering Design: Principles, Practice and Economics of Plant and Process Design*. Elsevier/Butterworth-Heinemann.

U.S. Bureau of Labor Statistics. (2023, April 25). Chemical plant and system operators. U.S.

Bureau of Labor Statistics. https://www.bls.gov/Oes/current/oes518091.htm

US Department of Energy. Fuel Cell Electric vehicles. Alternative Fuels Data Center: Fuel Cell Electric Vehicles. (n.d.). https://afdc.energy.gov/vehicles/fuel_cell.html

US Water Systems. (2023, 29). When do I change my RO membrane? https://uswatersystems.com/blogs/blog/when-do-i-change-my-ro-membrane#:~:text=The%20reverse%20osmosis%20membrane%20on,it%20longer%20than%20five%20years

US Water Systems. (n.d.). 60 GPM Polaris scientific ultraviolet disinfection system - UVA-60B. https://uswatersystems.com/products/60-gpm-polaris-scientific-ultraviolet-disinfection-system-uva-60b

Xu, Q., Zhang, L., Zhang, J., Wang, J., Hu, Y., Jiang, H., & Li, C. (2022). Anion Exchange Membrane Water Electrolyzer: Electrode Design, Lab-Scaled Testing System and Performance Evaluation. *EnergyChem*, 4(5), 100087. https://doi.org/10.1016/j.enchem.2022.100087

Zhao, D. B., Haijiang Wang, Hui Li, Nana (Ed.). (2015). PEM Electrolysis for Hydrogen Production: Principles and Applications. *CRC Press*. https://doi.org/10.1201/b19096